Stephen F. Austin State University

SFA ScholarWorks

Electronic Theses and Dissertations

Summer 6-26-2018

Steric Effects of Alkyl Ammonium Salts on the Combustion of Exchanged Smectite Clays

Celeste A. Keith
cak035@yahoo.com

Follow this and additional works at: https://scholarworks.sfasu.edu/etds

Part of the Analytical Chemistry Commons, Environmental Chemistry Commons, Inorganic Chemistry Commons, Organic Chemistry Commons, and the Physical Chemistry Commons
Tell us how this article helped you.

Repository Citation

Steric Effects of Alkyl Ammonium Salts on the Combustion of Exchanged
Smectite Clays

Creative Commons License

STERIC EFFECTS OF ALKYL AMMONIUM SALTS ON THE COMBUSTION OF
EXCHANGED SMECTITE CLAYS

By

C. A. KEITH, B.S. in Chemistry

Presented to the Faculty of the Graduate School of

Stephen F. Austin State University

In Partial Fulfillment

Of the Requirements

For the Degree of

Masters of Science in Natural Science

STEPHEN F. AUSTIN STATE UNIVERSITY

August, 2018

STERIC EFFECTS OF ALKYL AMMONIUM SALTS ON THE COMBUSTION OF
EXCHANGED SMECTITE CLAYS

By

C. A. KEITH, B.S. in Chemistry

APPROVED:

_____
Dr. Alyx S. Frantzen, Thesis Director

_____
Dr. Russell J. Franks, Committee Member

_____
Dr. J. Brannon Gary, Committee Member

_____
Dr. Kevin W. Stafford, Committee Member

_____
Pauline M. Sampson, Ph.D.
Dean of Research and Graduate Studies

ABSTRACT

Bomb calorimetry was explored as a new method for determining the cation exchange capacity (CEC) of clays. Smectite clays were modified with several alkyl ammonium salts varying in number of carbons and the spatial orientation of the carbons about the central nitrogen atom. The clays used, standards purchased from the Source Clay Repository, have CECs of 44, 80, 88, and 120 meq/100 g. Theoretically, the combustion energy of the organo-clays should be approximately the same for each salt. Any differences in energy would be due to the different structures of the salts and how they are oriented in the interlamellar region of the clay. The number of alkyl ammonium salts that bind to the negatively charged sites in the clay layers would represent the CEC of the clay. The orientation of the organic cation in the interlamellar region was examined using x-ray powder diffraction, which provides the spacing between the clay layers. The combustion energy data collected using bomb calorimetry was used to calculate the CEC of the clay by comparing the energy from the pure salts to determine the number of salt molecules intercalated into the clay. Since the pure salt and the clay have a one-to-one charge ratio, the number of salt molecules will directly represent the number of negatively charged sites on the clay which is the CEC of the clay.

TABLE OF CONTENTS

LIST OF FIGURES

LIST OF TABLES

LIST OF ABBREVIATIONS

Å Angstrom

CEC Cation Exchange Capacity

DDH_2O Distilled deionized water

meq Milliequivalents

SHCa-1 California hectorite clay

SWy-2 Wyoming clay

STx-1b Texas clay

SAz-1 Arizona clay

TEA Tetraethylammonium

HTMA Hexyltrimethylammonium

TPA Tetrapropylammonium

MTBA Methyltributylammonium

PTMA Phenyltrimethylammonium

DTMA Decyltrimethylammonium

HDTMA Hexadecyltrimethylammonium

T. Pent Tetrapentylammonium

ODTMA Octadecyltrimethylammonium

MTOA Methyltrioctylammonium

CHAPTER 1

Introduction

Bomb calorimetry was explored as a feasible method for determining the cation exchange capacity (CEC) of clays. Smectite clays were modified with alkyl ammonium salts that range from being very uniform and symmetrically substituted, to long chains that are very asymmetrically substituted. The number of alkyl ammonium salts that bind to the negatively charged sites in the clay layers is representative of the CEC of the clay. The energy released by the combustion reaction is strictly that of the salt. Since there is a one to one charge ratio between the salt and the clay, the energy release was used to calculate the CEC of the clay. Accurately knowing a clay's CEC, is useful in determining how the clay can be used in society and everyday life. The orientation of the organic cation in the interlamellar region was examined using x-ray powder diffraction, which provides the spacing between the clay layers. The objectives of this study were:

1. Determine CEC of smectites using bomb calorimetry
2. Examine steric interactions occurring between alkyl chains of ammonium salts intercalated into the clay with the aid of x-ray diffraction.
3. Determine optimal salt and clay combination to determine CEC.

LITERATURE REVIEW

Smectite describes a broad class of clays which are part of the phylloaluminosilicate mineral group. Smectites include hectorite, montmorillonite, nontronite, and many other clay species with the general formula $(Al_{3.15}Mg_{0.85})(Si_{8.00})O_{20}(OH)_4X_{0.85} \bullet nH_2O$, where X is a monovalent cation such as sodium, Na^+ (Newman 1987; Perrin, 2009). This research was conducted using mostly montmorillonite and one hectorite. Hectorite clay is similar to montmorillonite in that they are both phyllosilicates, but the general formula for hectorite is: $Na_{0.3}(Mg,Li)_3Si_4O_{10}(OH)_2$ where Na is the monovalent cation. Looking at the formula, for hectorite, an absence of Al and the addition of Li is seen (Hectorite Mineral Data). What contributes greatly to the usefulness of the clay is its cation exchange capacity, CEC, which refers to the number of charge sites found in a clay structure per mass of clay.

Figure 1 depicts the structure of smectite clay (Newman, 1987; van Olphen, 1979). The clay layers are composed of a tetrahedral, octahedral, tetrahedral (TOT) sequence of sheets separated by the interlamellar region (Odem, 1984). The tetrahedral portion of the sheet, depicted with purple dots in Figure 1, is comprised of silicon (Si^{4+}), or aluminum (Al^{3+}) cations. The octahedral sheet, depicted with red dots in

Figure 1, is comprised of aluminum (Al^{3+}), iron (Fe^{2+}), or magnesium (Mg^{2+}) cations.

These tetrahedral and octahedral sheets are connected together through oxygen atoms to

form TOT layers.
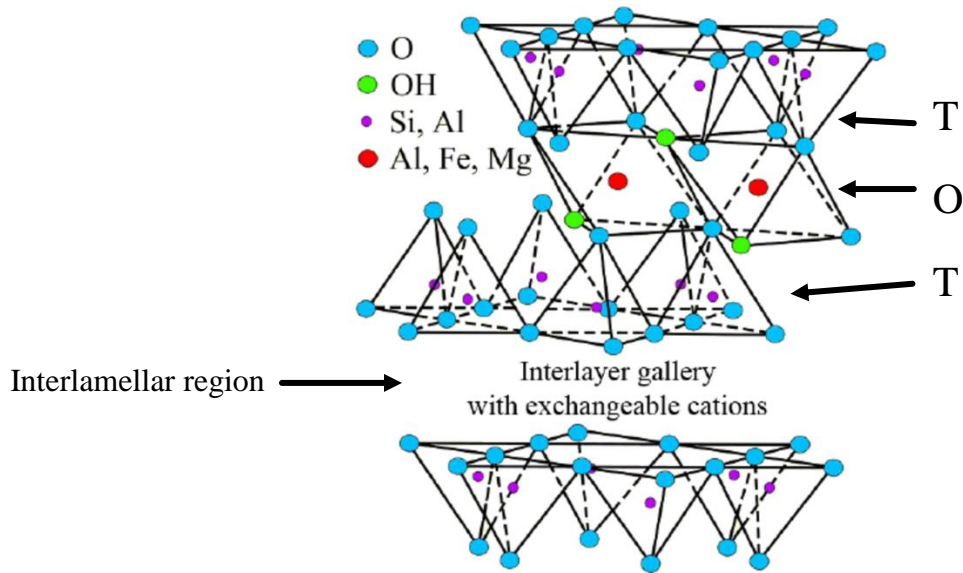
Figure 1. Structure of montmorillonite clay depicting the stacked layers of TOT layers (Steinmetz, 2007).

Ideally, silicon would occupy the tetrahedral layer and aluminum would occupy

the octahedral layer but, isomorphic substitutions occur during the formation of the clay;

aluminum (Al^{3+}) is substituted for silicon (Si^{4+}) in the tetrahedral sheet, Fe^{2+} or Mg^{2+}

can be substituted for Al^{3+} in the octahedral sheet, resulting in a net negative charge on

the clay (Newman, 1987). This negative charge in the clay layer allows for electrostatic

interaction to occur in the interlamellar region. Molecules of water along with cations

such as sodium (Na^+), calcium (Ca^{2+}), and magnesium (Mg^{2+}) freely exchange in the

interlamellar region due to this charge deficit (Rodríguez-Reinoso, 1991). The number of

negative charge sites on the clay is the clay's CEC. The CEC dictates the usefulness of

the clay in certain industrial applications. Clays can be used in anything from well

drilling to beauty products depending on this property. Clays with high CECs are more

structurally resilient than clays with lower CECs; this means that clays with higher CECs

can withstand drastic changes in ion concentration and size better than those with lower

CECs, while still maintaining their shape. At high concentrations of Na^+, the clay has

very useful swelling and hydration properties (Kloprogge, 1999).

Based on micrographs obtained using an electron microscope by Grim and Guven

(1978), smectite crystals can be as large as 2 μm and as small as 0.2 μm with an average

size of 0.5 μm. The individual crystal structures that make up the layers range in shape

from rhombic to hexagonal. This variation in size and shape of crystal structure gives the

clay a very large chemically active surface area if all of the conditions are ideal. During

formation of the clay, structural units fuse and interlock making them very difficult to

separate. These occurrences heavily impact the capacity of the clay to exchange ions,

clay viscosity, and fluid loss. Regardless of what interactions occur during formation,

smectite clay still has a large chemically-reactive surface area (displayed in Table 1).

The larger the surface area, the more interactions can take place within the layers of the

clay (Odem, 1984).

4

Table 1: Clays of interest and corresponding surface area for each (van Olphen, 1979).

Clay	Surface area (m^2/g)
SHCa-1	63.19
SWy-2	31.82
STx-1b	83.79
SAz-1	97.42

The hydration and dehydration of the interlamellar layer are also significant determining factors for how the smectite clay is used in industry. The degree of hydration is dependent on the species of exchanged ions, the size and shape of the ion and the magnitude and location of the layer charge of the adjacent silicate sheets (Odem, 1984). The interactions occurring between the layers of clay and the water molecules present (depending on the humidity level) yields highly organized layers of water in the interlamellar region. At high humidity levels, one to six layers of water can be present. The ions present and their tendency to hydrate dictate the thickness of the water layers that develop.

All of these properties can be utilized in different ways to customize the clay for whatever task the user is seeking to accomplish. Smectite clay is widely used as an adsorbent and catalyst for organic compounds, which are of large importance to the petroleum industry. Smectites interact well with organic compounds because of the various bonds that can be formed between the oxygen surfaces of the clay and the organic surfaces. Certain organic molecules that carry metals as complexes act as a sort of pillar structure between the layers of clay, propping them open and increasing interlamellar separation. This increases the catalytic activity of the interlamallar surface of smectite

which has a significant importance in petroleum cracking catalysts such as fluid catalytic cracking and hydrocracking (Eman, 2013). In recent years, smectite clays have been used more and more to absorb various organic and inorganic contaminants from industrial waste water (Teich-McGoldrick, 2015). A small amount of clay is added to the water, the contaminants are absorbed, and the clay is then removed from the water. Smectite clay can also be used to line landfills in an effort to prevent leaching of heavy metals or organic contaminants into ground water. Bentonite, a type of smectite clay, is used as a filler in pharmaceuticals. Due to its hydration characteristics, it can be made into a paste and used in face creams (Odom, 1984).

CHAPTER 2

Justification and Methodology

There are many methods for determining the CEC of a clay including ammonia

electrode, and x-ray diffraction. The ammonia electrode method was developed by

Busenberg and Clemency and involves exchanging the clay with ammonium ion (NH_4^+).

The NH_4-clay is suspended in distilled deionized water (DDH$_2$O) and monitored with an

ammonia electrode. Excess sodium hydroxide is added, converting the ammonium to

ammonia (Eq.1). The amount of ammonia detected is directly proportional to the CEC of

the clay.

$$Eq. 1: NH_4 - clay_{(suspension)} + NaOH_{(aq)} \rightarrow NH_{3(g)} + H_2O_{(l)} + Na - clay_{(suspension)}$$
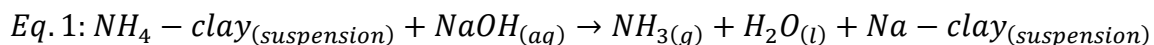
These values are compared to a standard curve developed using ammonium chloride

solutions and the concentrations of ammonia in the exchanged clay samples were

obtained using Equation 2.

$$Eq. 2: \qquad\qquad CEC = \frac{100c}{w \times 10^{-5}}$$

Where 100 represents the volume of water added to the clay, c represents the

concentration of ammonia in mol/L, w is the weight of the clay in grams and 10^{-5} is a

conversion factor (Busenberg, Clemency, 1973)(Borden, Giese, 2001). There are several

problems with this method, which lead to an accepted range of accuracy of ±20% of the known CEC (Busenberg, Clemency, 1973). When the clay is ground into a fine powder, not all of the pieces are uniform so not all of the ammonium ions are uniformly in contact with the hydroxide ions when introduced to the suspended clay. The result of the grinding means that not all of the ammonium ions are reacting to produce the ammonia gas at the same time, and in some cases not reacting at all. In order to get a signal from every ammonium ion on the surface of the clay, the probe would need to be submerged into solution for an undeterminable amount of time since the ammonia molecules are constantly being produced at an unsteady rate. This leads to inaccuracies in the results since more ammonium ions can be introduced into the system from the surrounding environment; in addition, the ammonia gas already produced from the reaction can possibly be counted multiple times. Another possible inconsistency with the current method is that the sodium hydroxide used, although it is very concentrated, might not have enough hydroxide to react completely with all of the ammonium ions. In addition, the electrode itself is very sensitive; at the end of the electrode is a Teflon membrane used to monitor concentration of ammonia in the environment at the surface of the suspension. This Teflon membrane can be damaged (scratched, cracked, or chipped) very easily, so poor results might occur. Also, when submerging the electrode into the suspended clay, it is important to make sure no air bubbles get trapped against the membrane. This phenomenon results in inaccurate results since the membrane is not making contact with the ammonia molecules produced.

The XRD method used x-ray diffraction to measure the distance between layers of clay. The clays are exchanged with the alkyl ammonium salts of interest. These alkyl ammonium salts were obtained by titrating commercially available alkyl amines dissolved in water-ethanol with either hydrochloric or formic acid. The exchange process for this method involves adding a calculated concentration of alkyl ammonium salt solution to the purified clay. Excess salt solution is washed with water-ethanol solution then pure ethanol (Lagaly, 1994). The clay samples are then air dried and prepped for XRD analysis. Next, the spacing between the layers of the exchanged clays is collected, and the number of alkyl salt molecules is calculated. This method is purely qualitative and provides a theoretical number of charge sites in the clay. Additionally, the equipment required is very expensive, must be properly maintained, and takes up a lot of space (Fernandez Gonzalez, Lagaly *et al*. 1976).

The method under investigation for determining CEC is to use bomb calorimetery to determine the combustion energy of alkyl ammonium exchanged clays. The clay itself will not combust, but, when exchanged with an alkyl ammonium salt, a combustion reaction will occur since there is organic matter present. Theoretically, there should be one ion per charge site in the clay. The total amount of energy solely depends on the number of carbons in the ammonium salt. This energy should be directly related to the number of charge sites in the clay.

In the bomb calorimetry method, the semi-micro bomb calorimeter is first standardized using benzoic acid. The sample is placed into the reaction vessel and

charged with oxygen, placed into the calorimeter, and the sample is combusted. The heat

released from this combustion reaction is recorded by the instrument and used to

calculate the energy release of the reaction. The heat of combustion of the pure salts was

also be determined. A comparison of the combustion of the salts and modified clays was

used to calculate the CEC. Since there is a one-to-one charge ratio between the salt and

the charge sites on the clay, the energy released from the combustion is coming from the

organic salt at those charge sites and will be representative of the number of charge sites

in the clay, which is the clay's CEC. At the end of the combustion process, upon opening

the vessel there will be two things remaining, water, and the incombustible material

which is the remaining clay. The combustion method should be a more efficient reaction

than the reaction of ammonium ions with hydroxide to produce ammonia and should give

less variability than in the previous method. Ideally, using the combustion method, the

accuracy range will narrow to $\pm10\%$ as opposed to the $\pm20\%$ of the ammonia electrode

method.

The organoclays were also analyzed using x-ray diffraction, which should give an

idea of how the ammonium salt is oriented between the TOT layers. Since these salts

have varying alkyl chains, how they are oriented in the interlamellar region will vary as

well as how many salt molecules are binding to the charge site in the clay. Additionally,

if there are long alkyl chains present, they might prevent other cations from binding to

neighboring charge sites, or form pseudo layers with neighboring chains. This process

was repeated with various combinations of alkyl ammonium ions and clays. The ions

10

varied from very symmetric (tetraalklyammonium) to less symmetric (trialkyl methyl; dialkyl dimethyl) to investigate if there are steric effects on the combustion energies (Mermut, 2001). This helped to give an idea of how the alkyl chains are interacting with the negative charge sites, and with each other, in the interlamellar region. Since these salts vary in the arrangement of these alkyl chains, the interlamellar region might be spaced differently depending on the salt present. For instance, if a salt has a very long alkyl chain, the chain might sterically inhibit other salt ions from interacting with the charge site due to overlap or blocking of the site. Finding the ideal orientation of substituents for each specific clay is vital for development of this method in order to ensure efficiency of determination (Perrin, 2009).

  X-ray diffraction crystallography (XRD) is a method of measuring the spacing between repeating layers in a structure; XRD was used to observe the distance between the top tetrahedral sheet of one TOT layer down to the top tetrahedral sheet of the TOT layer below it including the region called the interlamellar region or spacing. The thickness of the first TOT layer is then subtracted out to calculate the interlamellar region alone. A beam of incident radiation (X-ray) is directed onto the surface of the sample. Some of the radiation will strike atoms on the first layer, be diffracted then directed out at the same angle it originally struck the sample. Simultaneously, another beam is striking another atom on a lower layer (or the same layer) causing the same phenomenon. If these diffracted waves interfere constructively, a signal will be detected. If they interfere destructively no signal will be detected because the waves will cancel each other out.

11

The instrument uses this signal (constructive waves) to determine the spacing between the layers using Bragg's law (Equation 3) (Moore and Roberts, 1997). A schematic diagram is displayed in Figure 2. Where d (in the equation) represents the spacing between the layers (interlamellar region).

$Eq.3:$ $$2d\ sin\theta = n\lambda$$
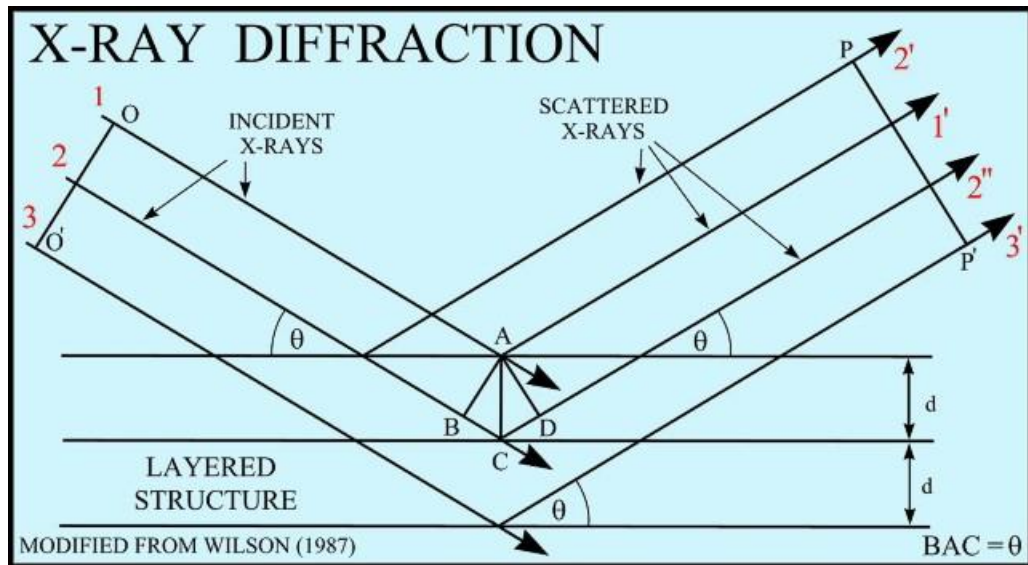
Figure 2: Visual representation of incident light rays interacting with layers of sample (Poppe, 2001).

Several salts and clays were examined throughout this research, starting with the materials already available, and expanding in the future when more are made available. Displayed in Table 2 are the proposed clays for this project along with their corresponding CEC in meg/100 g of clay, (Mermut, 2001). The clays are abbreviated with an 'S' for smectite, followed by the abbreviations for the states where they were

collected. The first clay listed is a hectorite, as indicated by the 'SH' abbreviation. The

clays of interest were chosen to represent a wide range of CEC from low to high. Since

in the combustion reaction the only combustible materials present are the alkyl chains of

the ammonium salt, and the CEC is representative of the number of negatively charged

sites on the clay surface, the clays with lower CECs will release a lower amount of

energy in the combustion. These clays are standard clays, so they have been very well

characterized which provides an excellent reference point for the research. The proposed

salts were chosen to observe whether or not the length and shape of the alkyl chain

effects the interaction of the nitrogen atom with the negative charge site on that clay. The

key to this project is to find the best combination of clay and salt in order to achieve the

most accurate CEC possible.

CHAPTER 3

Materials and Methods

Clays were purchased from the Source Clay Repository at Purdue University. The clays are listed in Table 2.

Purification

The initial step in the purification is sedimentation. The clay fraction of the sample is separated from the non-clay fraction through suspension. Approximately 50 grams were placed in large beakers and filled with distilled deionized water (DDH_2O), then placed on stir plates and allowed to stir for at least 4 hours. The suspension was then allowed to settle overnight. The next day, the supernatant was syphoned off into another beaker (decarb I beaker), while the remaining contents of the sedimentation beaker were suspended with water and allowed to stir for another day. The supernatant contains the clay that will go on to be purified. This process was repeated until the water added to the beaker for suspension was clear. The remaining content is the non-clay fraction that can be disposed of easily. The supernatant that is siphoned off from the sedimentation beaker is opaque in appearance and slightly more viscous than water; this is the unpurified clay.

Table 2: Proposed smectite clays with corresponding CEC values and their origin (Mermut, 2001)(van Olphen, 1979).

Clay	CEC (meq/100 g)	Source
SHCa-1	44	Red Mountain Andesite formation (pliocene)
SWy-2	80	Newcastle formation, (cretaceous)
STx-1b	88	Manning formation, Jackson group (eocene)
SAz-1	120	Bidahochi formation (pliocene)

The clay from sedimentation was then moved to the decarbonation I (decarb I) step. During the decarb I process, any carbonate species that remain after the suspension are removed. This step began with heating the suspended clay to 60-65° C while the pH was adjusted to 5 using 0.1 M HCl. All chemicals used were purchased from Sigma-Aldrich and were reagent-grade quality. The suspension was allowed to stir under these conditions for one hour and then cooled down to room temperature, excess NaCl was added, and the solution was left to settle overnight. The NaCl causes the clay to flock and collect at the bottom of the beaker allowing for the excess water to be removed easily. The remaining clay from decarb I was then put through a second decarbonation step (decarb II), which includes reheating the clay to 60-65° C for one hour with stirring. In this step, the clay is buffered to prevent readsorption of carbonates. At this temperature, acetic acid and sodium acetate are added to the clay. The quantities of materials added were determined by estimating how much clay was present in the beaker; 1.7 mL of acetic acid /g clay and 4.08 g of sodium acetate/g of clay are required for

decarb II. After the addition of the acetic acid and the sodium acetate, the clay was left to cool down to around 30-40 ° C where 3-4 spatula scoops of NaCl were added to cause flocculation. The clay was then left to cool to room temperature and was then centrifuged with additional scoops of NaCl added to each centrifuge bottle. The centrifuge used was a Beckman J2-HS, with a 4x1000 rotor. Centrifuging occurred at 7000 RPM at a temperature of 25°C for 20 minutes. After centrifuging, the water was decanted and the remaining clay in the bottle was resuspended with water and moved to metal removal.

In this step, all nonstructural metal ions are removed through oxidation and complexation with citrate. For the metal removal step, the clay was reheated to 50-60°C with stirring where sodium citrate and $NaHCO_3$ were added, based on the established amount of clay; 0.7g/g clay, and 0.08g/g clay, respectively. The clay was allowed to continue heating until it reaches 65° C when sodium dithionite was added scoopwise until the clay turned a milky white color; once achieved, the clay was left to cool to room temperature. The clay was then centrifuged, adding a scoop of NaCl to each centrifuge bottle. The supernatant was discarded and fresh water was added. This was repeated until the supernatant no longer smelled like sulfur (about 4-5 centrifugations). The clay was removed from the centrifuge bottles and resuspended using as little water as possible. The next step in the purification process was oxidation.

During the oxidation step, all excess organic material is removed from the clay. This step began with reheating the resuspended clay to 65° C with stirring, 30% H_2O_2

was then added to the clay (1 mL/g clay). The clay was the left to cool to room temperature and centrifuged one time with a scoop of NaCl added and then resuspended. The clay was saturated with NaCl (Na-clay) and was ready to be exchanged with the desired alkyl ammonium salt(s).

Exchange

The exchange process began with first determining the density of the clay. This was done by weighing an empty watch glass, adding an exact volume of the clay with a volumetric pipet and allowing the clay to dry either on the bench top or in a warm oven. Once dried the watch glass was weighed again to determine the mass of the dried clay present. This density was used to determine how much clay needed to be dispensed to produce an exact amount of dried, exchanged clay. The theoretical cation exchange capacity was then used to determine how much of the ammonium salt was required to provide a complete exchange of NaCl for the ammonium salt, 1.5 times the amount of salt required based on the charge ratio was added to the clay to ensure complete replacement of the NaCl. Displayed in Table 3 are the full names, and the purities of the salts used.

Table 3: Salts with corresponding number of carbons on alkyl chains exchanged with each clay.

Cation	# carbon atoms	Purity
Tetraethylammonium (TEA)	8	98+%
Hexyltrimethylammonium (HTMA)	9	98+%
Phenyltrimethylammonium (PTMA)	9	98+%
Tetrapropylammonium (TPA)	12	98+%
Decyltrimethylammonium (DTMA)	13	98+%
Methyltributylammonium (MTBA)	13	98+%
Hexadecyltrimethylammonium (HDTMA)	19	95%
Tetrapentylammonium (T.Pent)	20	99+%
Octadecyltrimethylammonium (ODTMA)	21	98%
Methyltrioctylammonium (MTOA)	25	97%

The amount of alkyl ammonium salt used was determined using Equation 4. The example calculation was for 10 g of exchanged clay MTBA-SHCa-1 using the known CEC and the molecular weight of the salt.

$$Eq.\,4 \qquad 10\;g\;exchanged\;clay \times \frac{44\;meq}{100\;g\;clay} \times \frac{1\;eq}{1000\;meq} \times \frac{1\;mol}{1\;eq} \times \frac{280.30\;g}{1\;mol}$$

$$= 1.23\;g\;MTBA$$

To ensure that all of the sodium ions were being replaced, an excess of the alkyl ammonium salt was added. The calculated mass (1.23 g using the example) was then multiplied by 1.5 to determine the final mass of MTBA required for SHCa-1. This same calculation was used to determine the mass of salt required for every clay. The appropriate amount of Na-clay was dispensed into beakers along with the required

amount of ammonium salt of interest and allowed to stir overnight, or at least four hours.

If needed, water was added in small quantities to facilitate stirring of the clay. After

stirring, the clay was allowed to settle for several hours or overnight. The water was

decanted, and the remaining clay was moved to dialysis tubing (MWCO 12,000-14,000

flat width: 45 mm), then placed in sufficiently large beakers filled with DDH_2O and

allowed to set for at least four hours or overnight. The water was poured off and fresh

water was added to the beakers when convenient. The dialysis tubing allows for

diffusion of the displaced Na^+ and Cl^- ions out of the clay and into the surrounding water

so it could be removed leaving behind only the desired alkyl ammonium salt. The

surrounding water was collected after about 3 or 4 water changes and tested with a few

drops of silver nitrate, if precipitation occurs in the water, halide ion was still present and

the water needed to be changed a few more times. If no precipitation occurs, then the

water needs to be changed one more time and the clay can be removed from the dialysis

tubing and poured onto drying plates. Once all the clay has been dried, it was scraped off

of the plates using a razor blade and a spatula and placed into appropriately labeled

storage containers. This dried clay was then ready for analysis using the semi micro
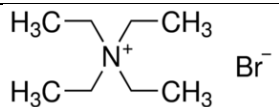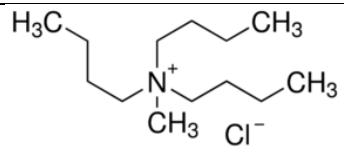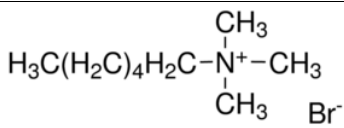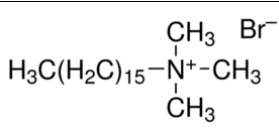
bomb calorimeter.

XRD
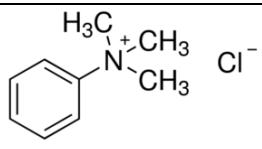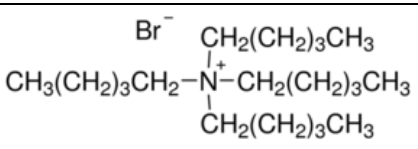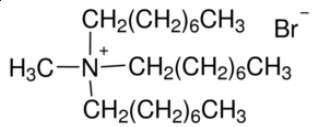
X-ray diffraction was done on each of the alkyl-ammonium clays to determine

how the salt was oriented in the interlamellar region of the clay. Comparison of how the

interlamellar spacing of the different salts on each clay helps describe how the salts are setting in the interlamellar region of the clay. This interlamellar spacing can give evidence of chain overlap and other hindering orientations that might be blocking other salts from interacting with the charge sites. The XRD used was a Bruker D8 Advance. The parameters under which the samples were analyzed are displayed in Table 4. All samples were prepared as randomly oriented powders. The individual samples were finely ground using a mortar and pestle and then placed into the sample holder of the XRD. The sample was smoothed flat, flush with the sample holder. The sample holder was then loaded into the instrument and the analysis was performed. From this, the interlamellar spacing was determined. Parameters were set using the Bruker XRD Wizard software and the instrument was run with Bruker Diffrac plus XRD Commander version 2.6.1. Once collected, the data was analyzed using Bruker Diffrac Eva version 3.1. The interlamellar spacing offers an idea of how the salt molecules are situated in the interlamellar region of the clay. As the chains of the salts get longer, there is a hig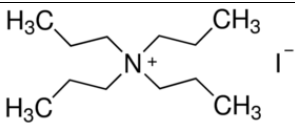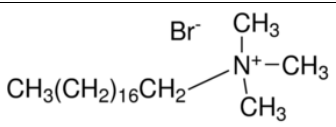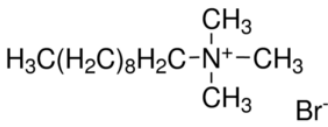h risk of pseudo layering occurring, which is a phenomenon where the long carbon chains overlap each other and drastically increase the interlamellar spacing by pushing the clay layers apart. This can result in charge sites being blocked preventing other salt molecules from interacting with the clay, leading to an inaccurate CEC calculation. Structure of the hydrocarbon chains around the central nitrogen atom greatly contributes to how the salt ion fits between the TOT layers in the interlamellar region of the clay; this information is displayed in Table 5.

Table 4: Bruker D8 Advanced XRD parameters.

Detector	Lynx Eye
Mode	Locked Couple/Constant Scan
Scan Axis	$2\Theta/\Theta$
Scan Range	$2.0°\text{-}15.0°$
Time per Step	1 second
Step Size	$0.05°$
Run at	40kV and 20mA
Source	Cu Kα

Table 5: Each alkyl ammonium salt used with its corresponding structure (MilliporeSigma).

Salt	Structure	Salt	Structure
TEA		MTBA	
HTMA		HDTMA	
PTMA		T.Pent	
TPA		ODTMA	
DTMA		MTOA	

Bomb Calorimeter Operation (Semi-Micro)

A Parr 6725 Semimicro Calorimeter fitted with a Parr 6772 Calorimetric Thermometer/Data Acquisition System was used to determine the energy of combustion of the samples. The reaction vessel (bomb) was a Model 1109A. The bomb was first standardized using benzoic acid pellets before any clay samples were analyzed. The pellets used were purchased from Parr Instruments. This benzoic acid was regent grade; the exact heat of combustion was known, and the masses of the pellets are all very similar (approximately 0.2 g). The benzoic acid pellet and 10 cm of fuse wire were placed into the reaction vessel and pressurized with 30 atm of O_2. The purpose of standardizing the instrument was to determine the heat capacity of the calorimeter. The reaction vessel was placed into a dewar flask held in the calorimeter which was filled with 450 mL of water before finally connecting the lead wires. The parameters for the sample were entered into calorimeter and the sample was combusted and results obtained.

Depending on the ammonium salt used, about 0.2 g of clay was either pressed into a pellet or loosely placed into the sample pan of the bomb calorimeter; some exchanged clays would not press into pellets, so those samples were loosely placed into the sample pan for analysis. Some samples would not combust as there was not enough salt present. These samples were analyzed by spiking the sample with benzoic acid. The mass remained at approximately 0.2 g, half being the clay sample and the other half benzoic acid. The heat provided by the benzoic acid was subtracted from the total heat produced. The procedure for the salt-clay samples were the same as the standardization procedure

with one exception: the benzoic acid was replaced with the salt-clay sample (Parr Operations Manual, 2007).

Bomb calorimeter operations (Standard Vessel)

A Parr Model 1331 Oxygen Bomb Calorimeter fitted with a Parr 6772 Calorimetric Thermometer/Data Acquisition System was used to obtain the heat of combustion for the pure alkyl ammonium salts. The reaction vessel used was a Model 1108Cl. This vessel is designed with superior corrosion resistance to the halogen acids released during combustion. The process was similar but a standard bomb calorimeter was used instead of the semi-micro. There were two standardizations completed for the standard vessel: one for the bomb calorimeter itself and another for the gelatin capsules used to hold the sample for analysis. The pure salts could not be pressed into pellets, so instead they were placed into size 00 gelatin capsules for analysis. The capsules were obtained from a local pharmacy. The heat contributed by the capsules was subtracted from the gross heat of the reaction. Sample sizes for the standard bomb calorimeter were approximately 0.8 g. (Parr Operations Manual, 2008).

CHAPTER 4

Results and Discussion

After the energies of both the pure salts and the samples were obtained, the CEC of the exchanged clay was calculated using Equation 4. The energies of the pure salts first had to be converted form cal/g to cal/mol. An example of how the CEC for STx-1 was calculated using the data from the DTMA-STx-1 sample is given in Equation 5. Table 6 displays the average energy of the pure salts, along with standard deviation, and converted energy in cal/mol. Table 7 displays all four clays used, all 10 alkyl ammonium salts of interest along with the corresponding heats of combustion in cal/g for each salt-clay combination.

Table 6: Average heats of combustion for pure salts, with corresponding standard deviations.

Pure Salts	Average (cal/g)	Standard Deviation (cal/g)	Energy in (cal/mole) of Salt
TEA	5445.945	87.25	1400479
HTMA	6981.767	71.83	1565033
PTMA	7528.884	145.18	1293161
TPA	5753.037	100.43	1802254
DTMA	7978.185	360.54	2236206
MTBA	7255.296	195.83	2033659
HDTMA	7895.207	230.39	2877487
T.Pent	8427.486	275.55	3189719
ODTMA	8118.855	167.90	3186813
MTOA	8360.388	1406.45	3750721

$$Eq.\,4: \quad \frac{Average\; \Delta H_{comb.} clay - salt\left(\frac{cal}{g}\right)}{Average\; \Delta H_{comb.}\; pure\; salt\left(\frac{cal}{mol}\right)} \times \frac{1eg}{1mol\; salt} \times \frac{1000meq}{1eq} \times 100g$$

$$= \frac{meq}{100g\; clay}$$

$$Eq.\,5: \quad \frac{1319.996\left(\frac{cal}{g}\right)}{2236205\left(\frac{cal}{mol}\right)} \times \frac{1eg}{1mol\; salt} \times \frac{1000meq}{1eq} \times 100g = \frac{59.028\; meq}{100g\; clay}$$

Table 7: All clay and salt combinations with their corresponding average heats of combustion.

Salt	Number of Carbons	SHCa-1 (cal/g)	SWy-2 (cal/g)	STx-1b (cal/g)	SAz-1 (cal/g)
TEA	8	544.887	663.716	895.207	985.671
HTMA	9	949.807	1049.202	765.347	1187.225
PTMA	9	739.374	369.874	669.921	1052.126
TPA	12	1219.261	1359.343	512.386	644.392
DTMA	13	1362.777	1385.055	1319.996	1990.921
MTBA	13	1154.437	1348.676	1115.332	1502.676
HDTMA	19	2593.935	2539.833	2731.463	4043.315
T. Pent	20	1869.394	1875.441	1451.737	1814.667
ODTMA	21	2813.820	3898.068	3814.961	3713.208
MTOA	25	3338.900	2987.421	2730.935	3989.862

SHCa-1

The average heats of combustion for all 10 exchanged SHCa-1 samples along with corresponding standard deviations are displayed in Table 8. All percent errors were calculated with respect to the accepted CECs provided from the Source Clay Repository.

Table 8: Average heat of combustion for exchanged SHCa-1 samples along with corresponding standard deviations, calculated CECs and percent errors.

Salt	Number of Carbons	Average heat of combustion (cal/g)	Standard Deviation (cal/g)	Calc. CEC (meq/100g clay)	Percent errors
TEA	8	544.887	166.274	38.91	11.57
HTMA	9	949.807	71.853	60.69	37.93
PTMA	9	739.374	242.847	57.18	29.94
TPA	12	1219.261	403.487	67.65	53.75
DTMA	13	1362.777	77.340	60.94	38.50
MTBA	13	1154.437	52.101	56.77	29.02
HDTMA	19	2593.935	71.756	90.15	104.88
T. Pent	20	1869.394	49.931	58.61	33.20
ODTMA	21	2813.820	98.907	88.30	100.67
MTOA	25	3338.900	157.379	89.02	102.32

The lowest percent errors came from TEA, PTMA, and MTBA, although only TEA yielded a percent error less than 20% with 11.57%. The standard deviations vary widely across the salts with some being over ±100 cal/g. The salt with the lowest percent error had the second highest standard deviation with 166.274 cal/g. The large percent errors are most likely due to spiking the sample which involves adding benzoic acid in order to achieve a combustion reaction. When a sample is spiked, half of mass is the sample and the other half is benzoic acid. The salt TEA is actually the smallest molecule

with the lowest number of carbons, and this clay, SHCa-1, has the lowest CEC of the

clays examined with 44 meq/100g clay. This meant that there was most likely not

enough organic material present in the sample to produce enough energy to generate a

measurable temperature change, yielding a lowest percent error, but a high deviation.

Theoretically, as long as the salts have a similar number of carbon-hydrogen bonds, they

should release the same amount of energy. The salts possessing 8-9 carbons have similar

energies except for PTMA, phenyltrimethyl ammonium, which is lower. This salt is the

only salt with a ring system, all of the other salts are aliphatic compounds. The

introduction of double bonds reduces the number of carbon-hydrogen bonds, lowering the

overall combustion energy of the sample. This is seen for all the PTMA-clay samples.

The average heats of combustion for each salt-SHCa-1 sample in relation to the number

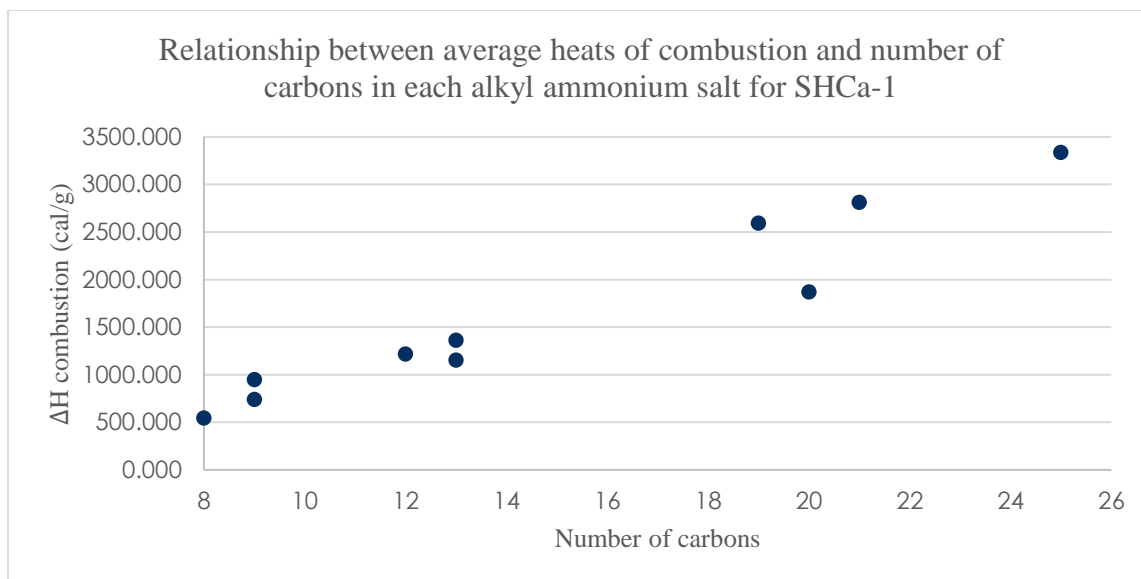of carbons of the alkyl chains are displayed in Figure 3.

Figure 3: Representation of the relationship between average heats of combustion and number of carbons in each alkyl ammonium salt for SHCa-1.

As seen in Figure 3, as the number of carbons present in the sample increases, so does the average heat of combustion. Graphical representation of the relationship between interlamellar spacing and the number of carbons on the alkyl chain of the ammonium salt for all exchanged SHCa-1 samples is displayed in Figure 4. Figure 4 provides evidence that the clay layers expand and change to accommodate the increase in number of carbons in the chain of the alkyl ammonium salt.
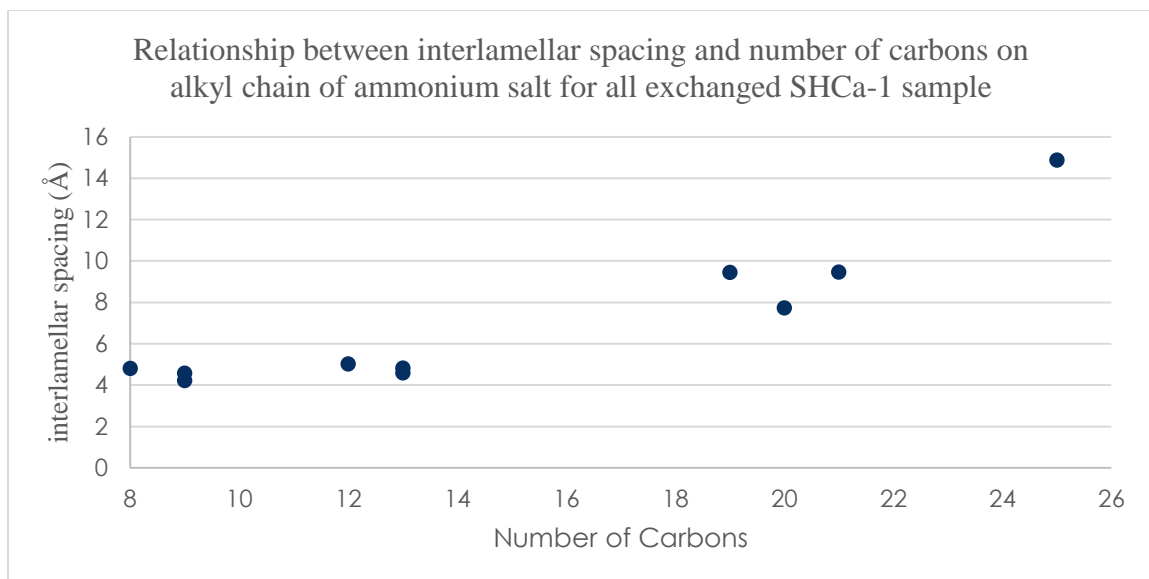
Figure 4: Representation of the relationship between interlamellar spacing and number of carbons in each alkyl ammonium salt for SHCa-1.

SWy-2

The average heats of combustion for all 10 exchanged SWy-2 samples along with corresponding standard deviations are displayed in Table 9.

Table 9: Average heat of combustion for exchanged SWy-2 samples along with corresponding standard deviations.

Salt	Number of Carbons	Average heat of combustion (cal/g)	Standard Deviation (cal/g)	Calc. CEC (meq/100g clay)	Percent errors
TEA	8	663.72	399.89	47.392	40.76
HTMA	9	1049.20	35.56	67.040	16.20
PTMA	9	369.87	275.34	28.602	64.25
TPA	12	1359.34	40.44	75.420	5.73
DTMA	13	1385.05	75.17	61.938	22.58
MTBA	13	1348.68	57.91	66.320	17.10
HDTMA	19	2539.83	34.03	88.266	10.33
T. Pent	20	1875.44	119.66	58.796	26.50
ODTMA	21	3898.07	158.89	122.319	52.90
MTOA	25	2987.42	25.54	79.649	0.44

The three salts that produced the lowest percent errors are MTOA, TPA, and HDTMA with percentages of 0.44, 4.73, and 10.33, respectively. All three of these were a vast improvement over the ±20% of the ammonia electrode method, while MTOA was the lowest with an excellent percentage of < 1%. Graphical representation of the relationship between the number of carbons and the average heat of combustion for all SWy-2 samples is displayed in Figure 5.
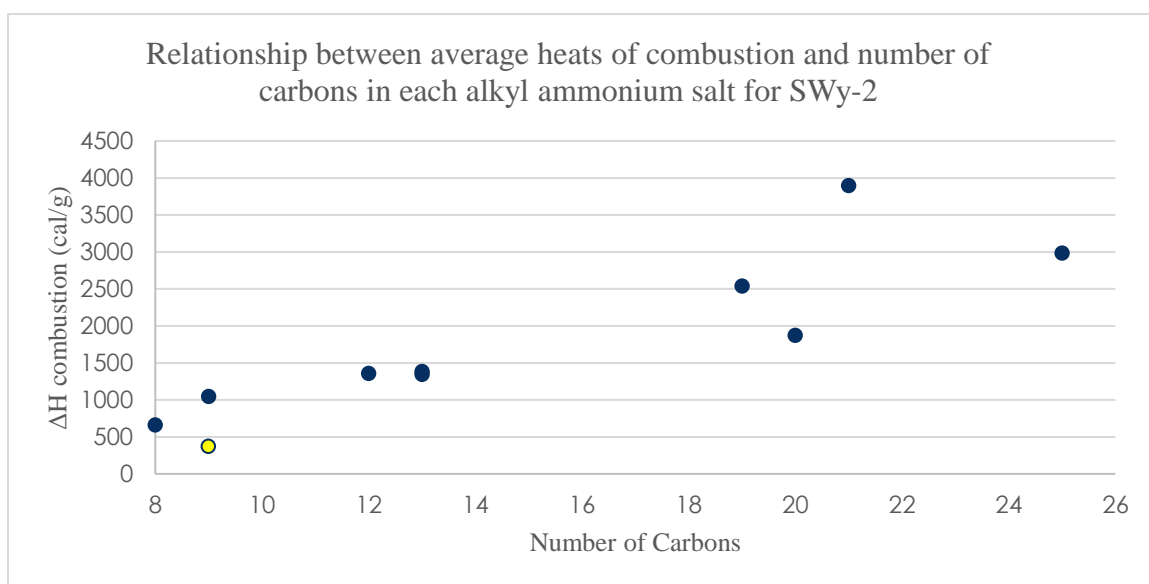

Figure 5: Representation of the relationship between average heats of combustion and number of carbons in each alkyl ammonium salt for SWy-2 with a yellow mark representing PTMA.

The same trend is seen with the SWy-2 that was seen with the SHCa-1 samples: as the number of carbons on the salt increases, that energy released form the combustion increases. The yellow mark represents the PTMA sample which was substantially lower than the surrounding values due to the presence of double bonds. Additionally, the same

trend for the interlamellar spacing of the exchanged SWy-2 samples is seen in Figure 6

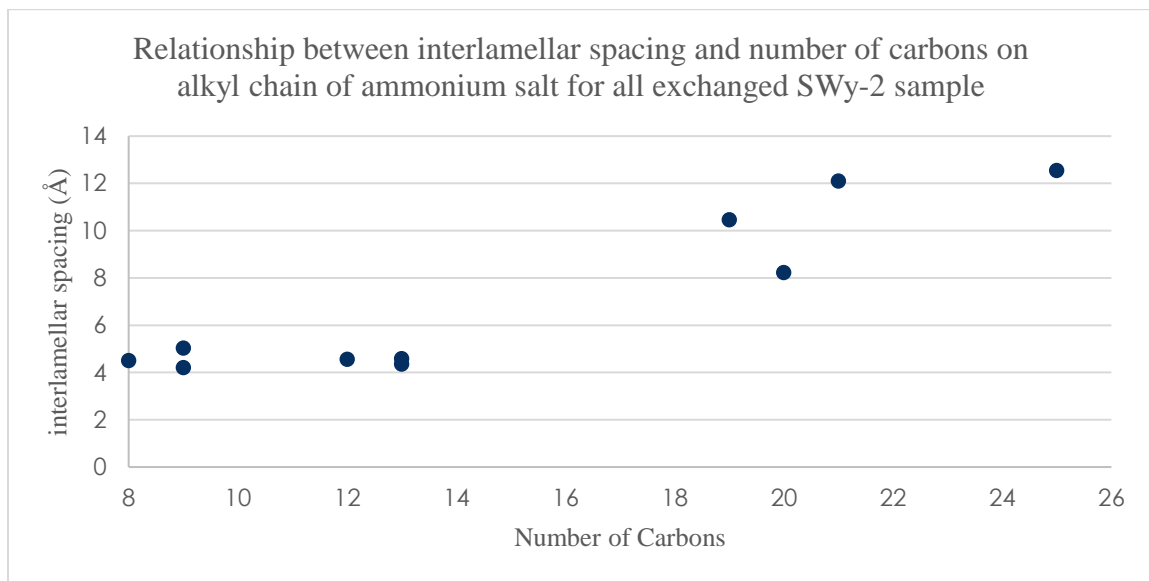that was seen with the exchanged SHCa-1 samples.

Figure 6: Representation of the relationship between interlamellar spacing and number of carbons in each alkyl ammonium salt for SWy-2.

STx-1b

The average heats of combustion for all 10 exchanged STx-1b samples along with

corresponding standard deviations are displayed in Table 10.

Table 10: Average heat of combustion for exchanged STx-1b samples along with corresponding standard deviations.

Salt	Number of Carbons	Average heat of combustion (cal/g)	Standard Deviation (cal/g)	Calc. CEC (meq/100g clay)	Percent Error
TEA	8	895.207	157.270	63.921	27.36
HTMA	9	765.347	246.740	48.903	44.43
PTMA	9	669.921	188.844	51.805	41.13
TPA	12	512.386	386.439	28.430	67.69
DTMA	13	1319.996	9.607	59.028	32.92
MTBA	13	1115.332	41.583	54.840	37.68
HDTMA	19	2731.463	67.560	94.925	7.87
T. Pent	20	1451.737	46.966	45.513	48.28
ODTMA	21	3814.961	103.256	119.711	36.04
MTOA	25	2730.935	49.353	72.811	17.26

According to the calculated percent errors for STx-1b, the salts best suited for CEC determination in this clay are HDTMA, MTOA, and TEA with percent errors of 7.78, 17.26, and 27.36, respectively. The best error was found using HDTMA (hexadecyltrimethyl) with three methyl groups and one long 16 membered chain situated around the central nitrogen atom. Graphical representation of the relationship between the number of carbons and the average heat of combustion for all STx-1b samples is displayed in Figure 7. The relationship between interlamellar spacing and number of carbons is displayed in Figure 8.
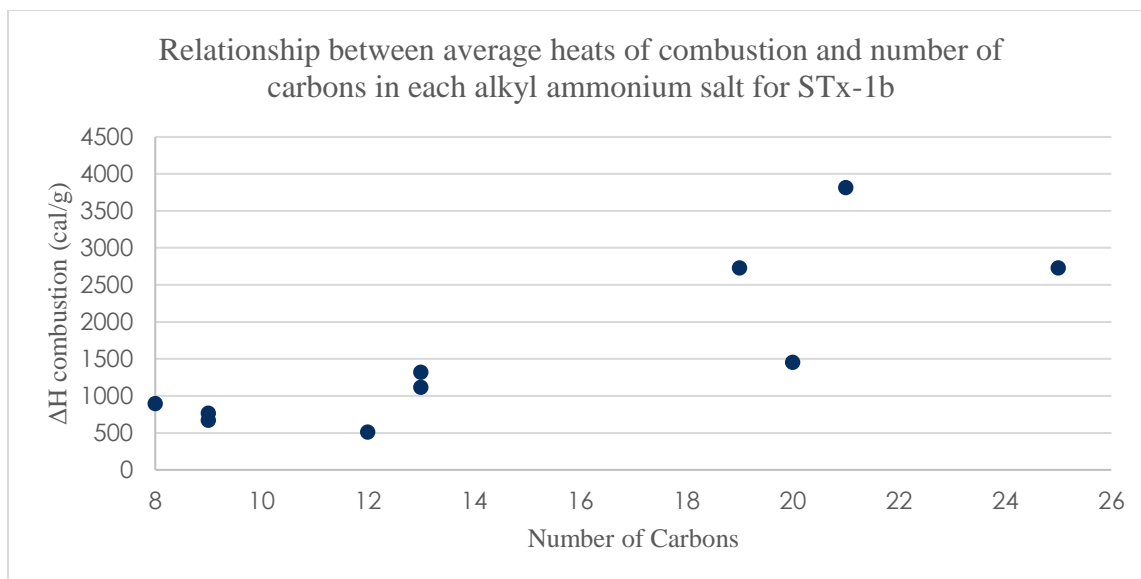
Figure 7: Representation of the relationship between average heats of combustion and number of carbons in each alkyl ammonium salt for STx-1b.
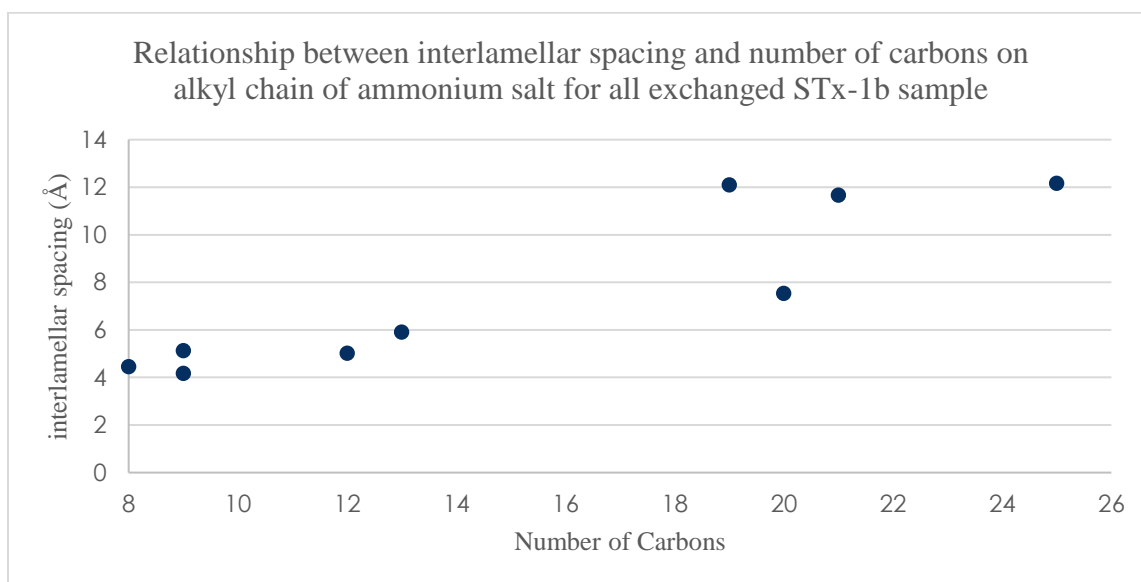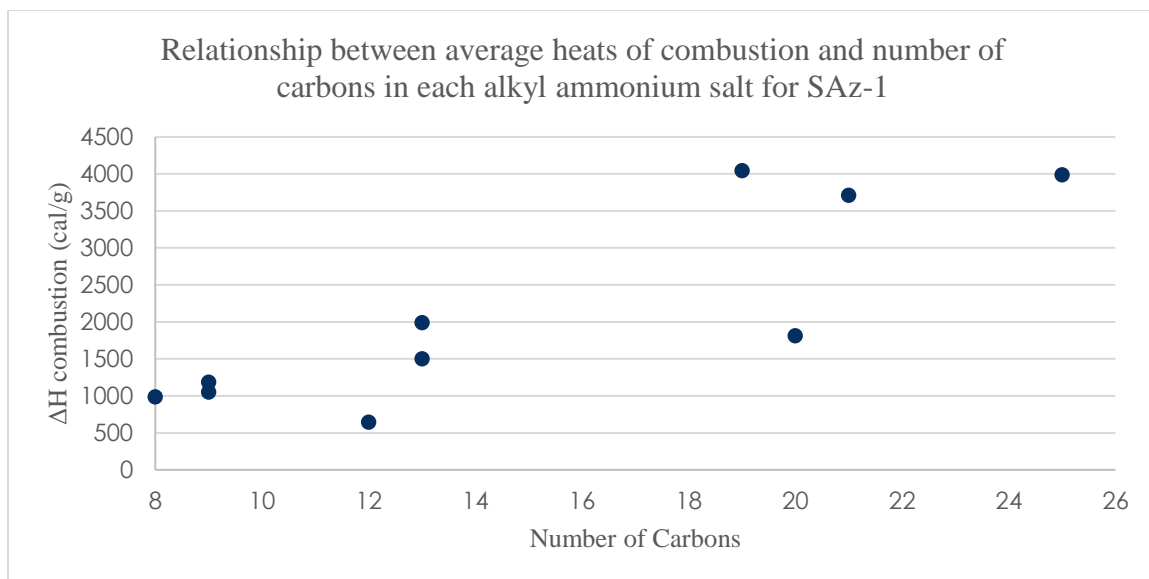

Figure 8: Representation of the relationship between interlamellar spacing and number of carbons in each alkyl ammonium salt for STx-1b.

For STx-1b, the positive trend that was very obvious with the previous clays is not there, although there still is a slightly positive correlation of the data. This is evidence that the clay is not affected as much by the increase in carbons of the alkyl ammonium salt. While the distribution of charge sites on the clay surface is random, with the increase in the number, they will be closer together. This would most likely result in the cations having to sit 'up right' instead of laying down flat.

SAz-1

The average heats of combustion for all 10 exchanged SAz-1 samples along with corresponding standard deviations are displayed in Table 11. The SAz-1 clay has the highest CEC of 120 meq/100g of the clays used. The three salts that yielded the three lowest percent errors were: ODTMA, MTOA, and HDTMA which percentages of, 2.90, 11.35, and 17.10, respectively. The lowest percentage came from the octadecyltrimethyl ammonium exchanged clay. The relationship between average heats of combustion and number of carbons is displayed in Figure 9. Representation of the relationship between interlamellar spacing and number of carbons in each alkyl ammonium salt for SAz-1. Is displayed in Figure 10.

Table 11: Average heat of combustion for exchanged SAz-1 samples along with corresponding standard deviations.

Salt	Number of carbons	Average heat of combustion (cal/g)	Standard Deviation (cal/g)	Calc. CEC (meq/100g clay)	Percent Error
TEA	8	985.671	159.701	70.38	41.35
HTMA	9	1187.225	58.863	75.86	36.78
PTMA	9	1052.126	120.319	81.36	32.20
TPA	12	644.392	538.610	35.75	70.21
DTMA	13	1990.921	39.784	89.03	25.81
MTBA	13	1502.676	12.569	73.89	38.42
HDTMA	19	4043.315	40.064	140.52	17.10
T. Pent	20	1814.667	34.117	56.89	52.59
ODTMA	21	3713.208	511.331	116.52	2.90
MTOA	25	3989.862	61.347	106.38	11.35

Displayed in Figures 11-20 is the data collected for the combustion energies of each salt in relation to the known CEC of each clay. All heats of combustion are recorded in cal/g, and all CECs are recorded in meq/100g of clay. In general, there should be a linear increase in energy as the CEC increases.

Figure 9: Representation of the relationship between average heats of combustion and number of carbons in each alkyl ammonium salt for SAz-1.
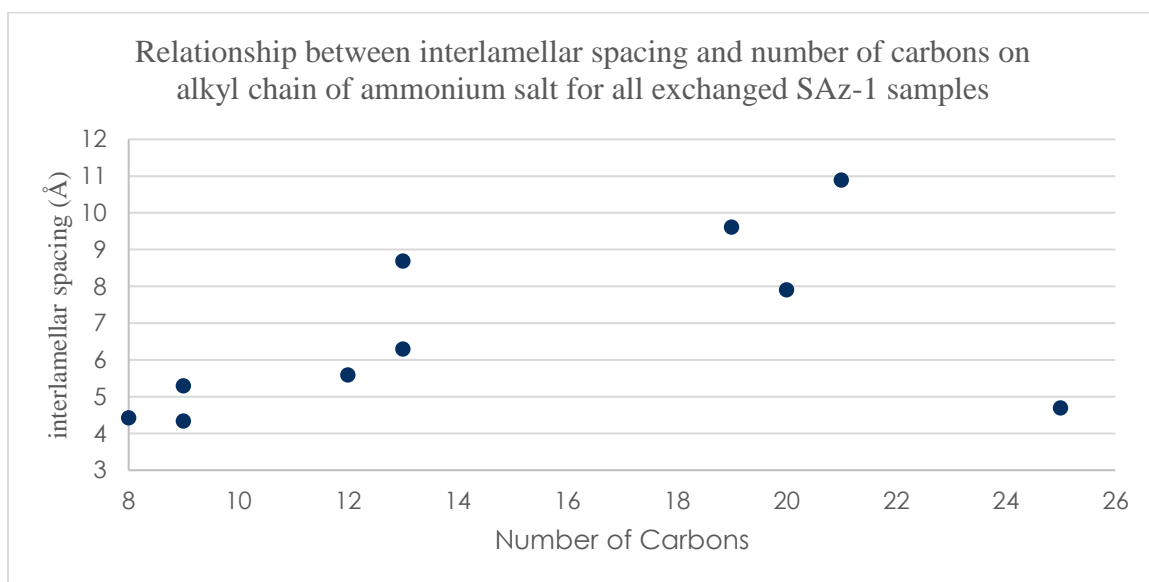

Figure 10: Representation of the relationship between interlamellar spacing and number of carbons in each alkyl ammonium salt for SAz-1.
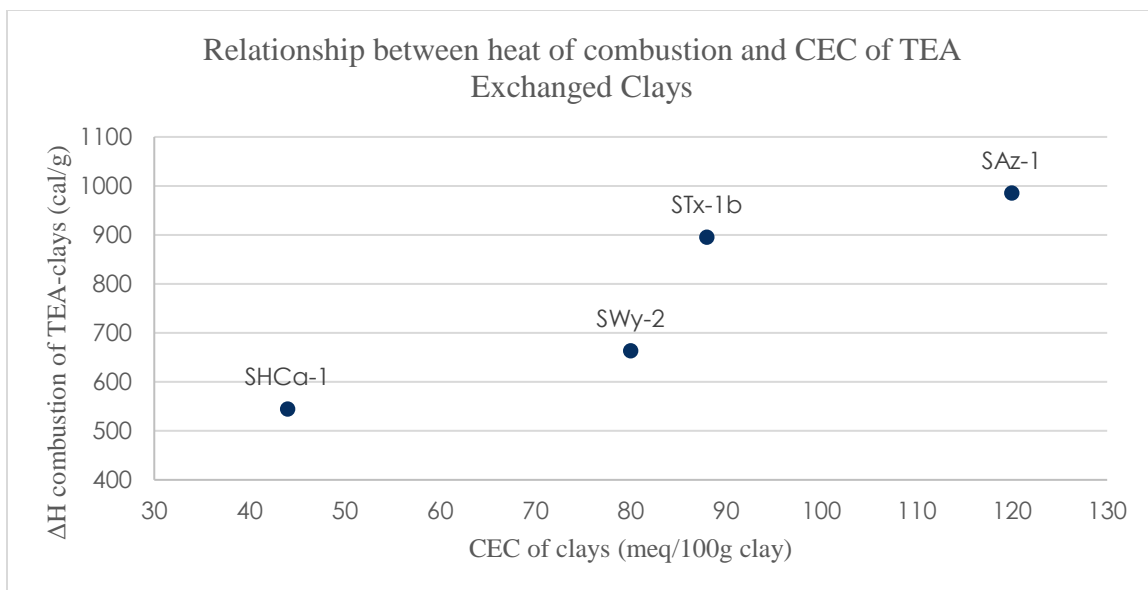
Figure 11: Average heats of combustion for all 4 TEA exchanged clays with respect to the accepted CEC of each clay in ascending order.
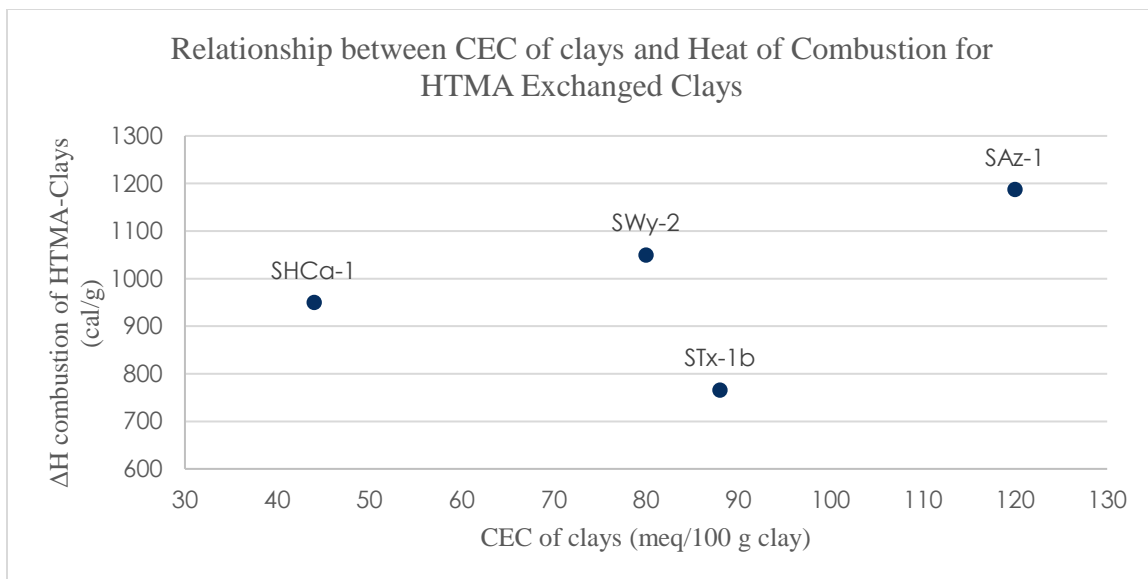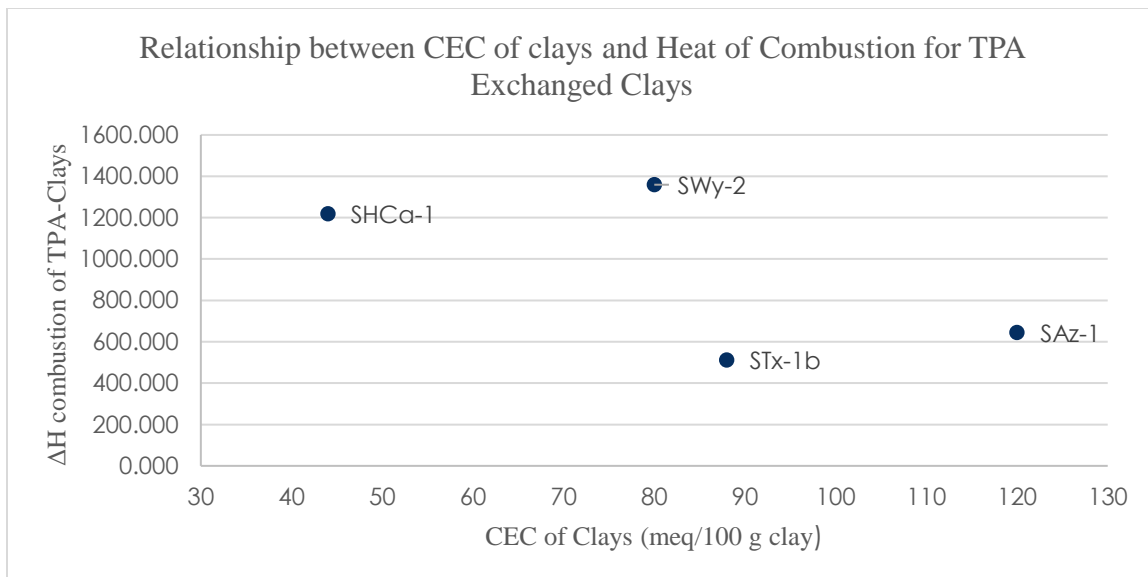

Figure 12: Average heats of combustion for all 4 HTMA exchanged clays with respect to the accepted CEC of each clay in ascending order.

Figure 13: Average heats of combustion for all 4 TPA exchanged clays with respect to the accepted CEC of each clay in ascending order.
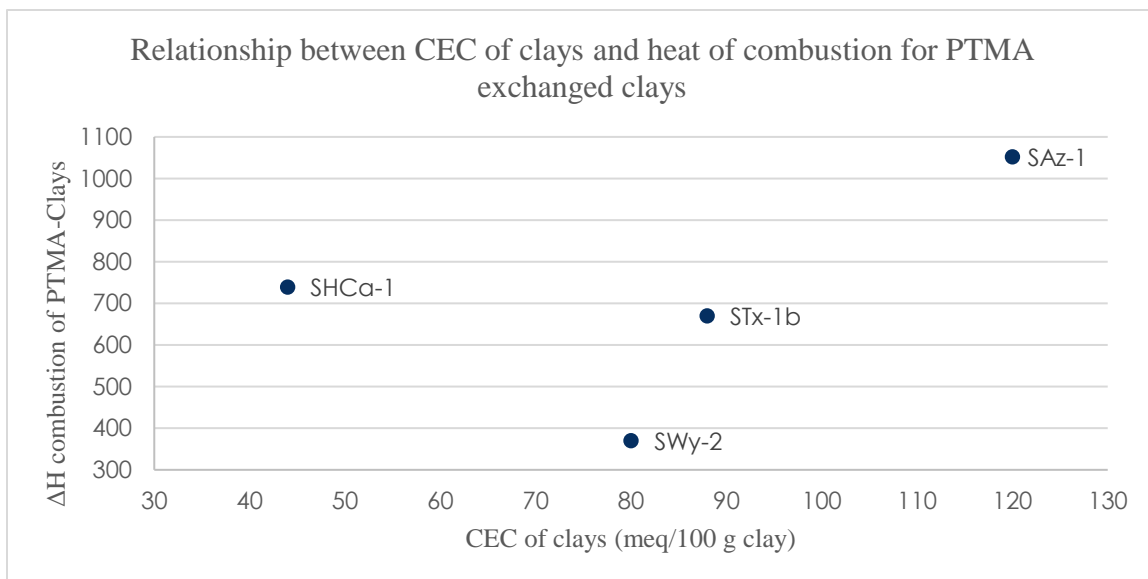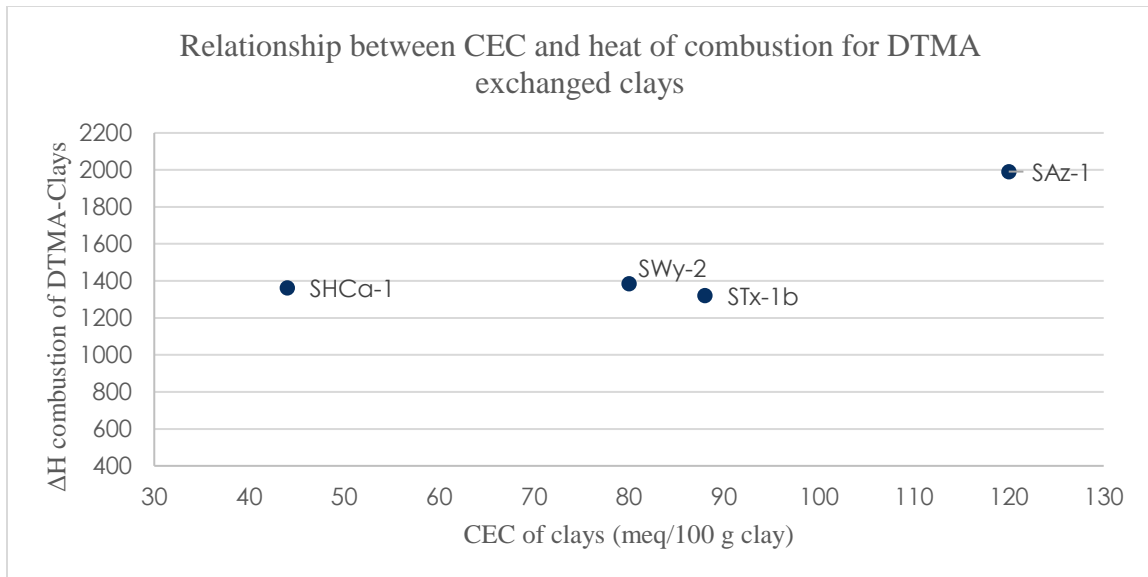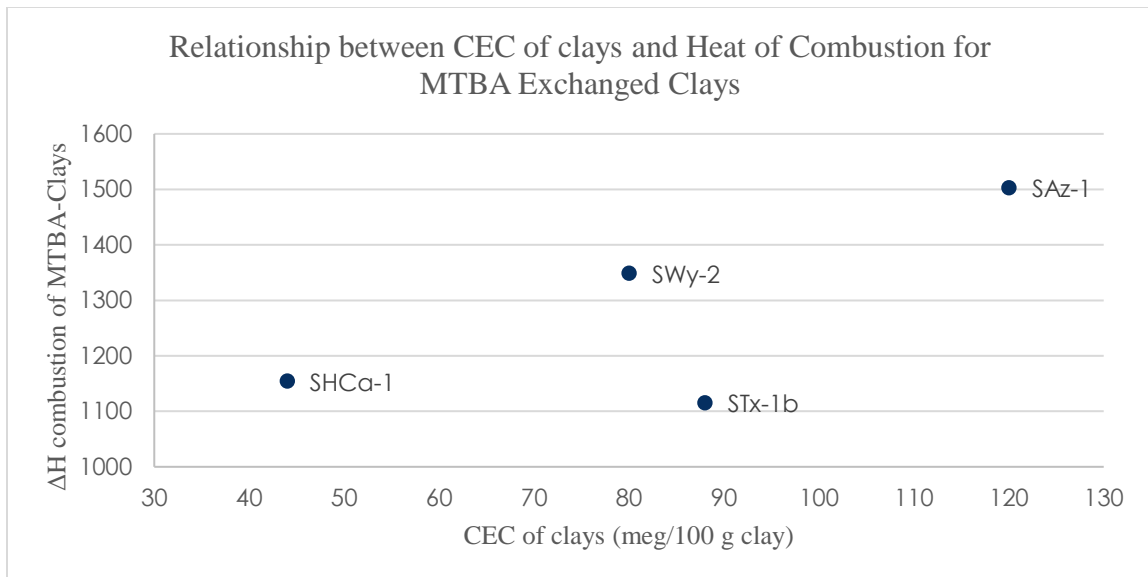

Figure 14: Average heats of combustion for all 4 PTMA exchanged clays with respect to the accepted CEC of each clay in ascending order.

Figure 15: Average heats of combustion for all 4 DTMA exchanged clays with respect to the accepted CEC of each clay in ascending order.

Figure 16: Average heats of combustion for all 4 MTBA exchanged clays with respect to the accepted CEC of each clay in ascending order.
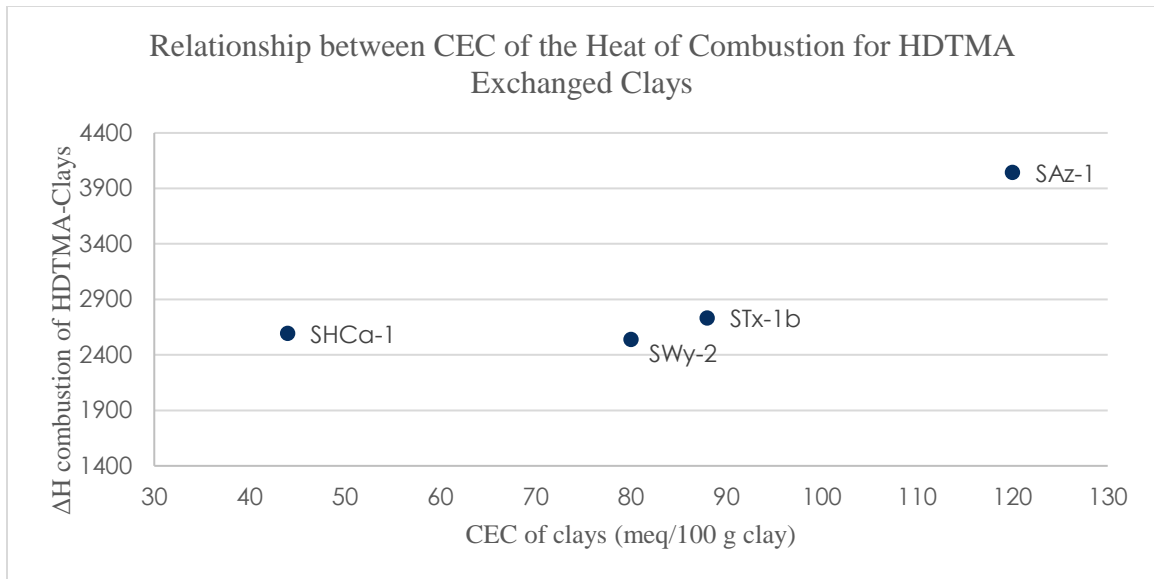
Figure 17: Average heats of combustion for all 4 HDTMA exchanged clays with respect to the accepted CEC of each clay in ascending order.
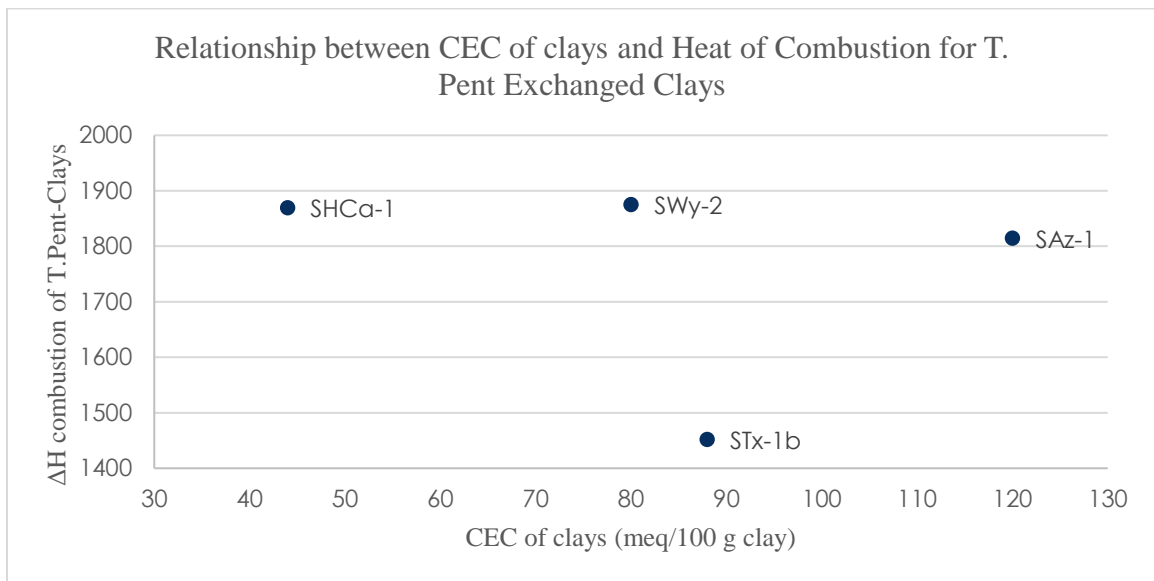

Figure 18: Average heats of combustion for all 4 T. Pent exchanged clays with respect to the accepted CEC of each clay in ascending order.
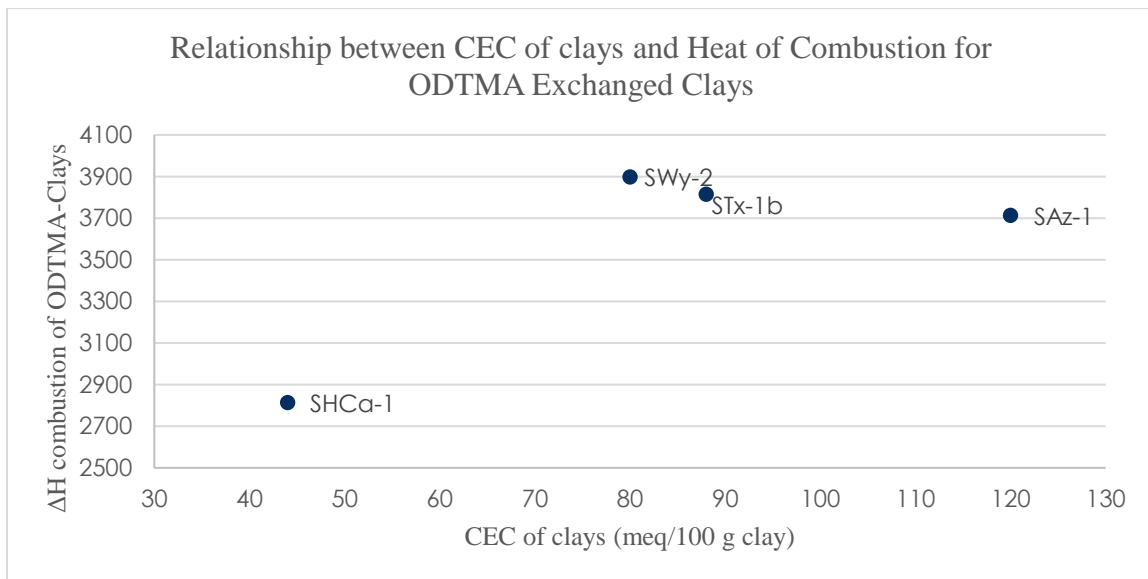
Figure 19: Average heats of combustion for all 4 ODTMA exchanged clays with respect to the accepted CEC of each clay in ascending order.
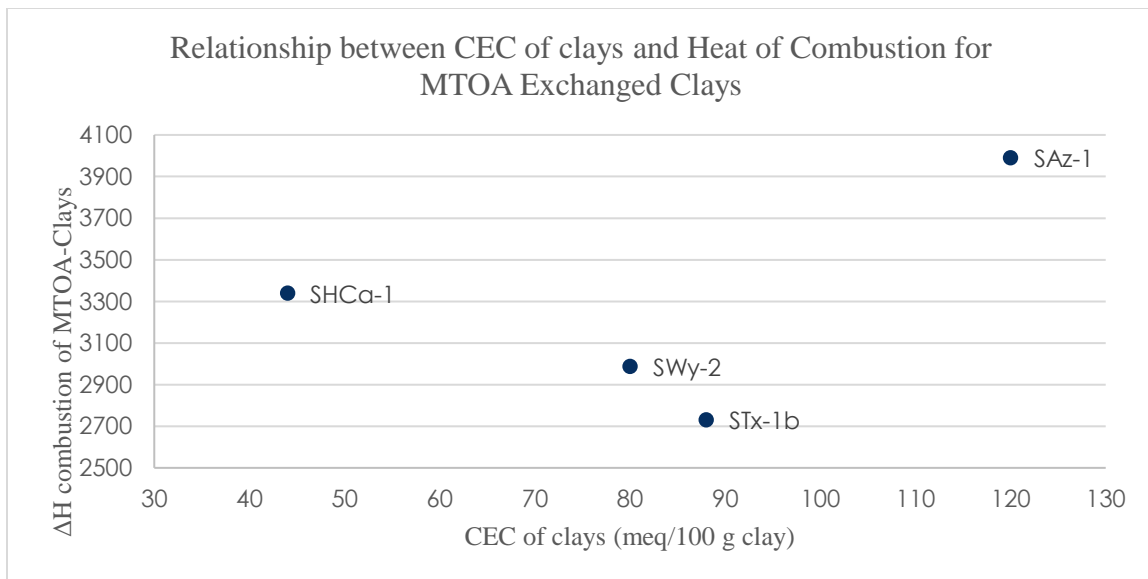

Figure 20: Average heats of combustion for all 4 MTOA exchanged clays with respect to the accepted CEC of each clay in ascending order.

Displayed in Table 11 are the interlamellar spacing for all salt-clay combinations, and in Figures 22-32 are the relationships between interlamellar spacing (in Å) and CEC of each salt-clay combination arranged in ascending order based on number of carbons. The XRD provides the layer thickness from the top of one TOT layer to the next. To calculate just the interlamellar spacing, the average thickness of a clay layer (9.8 Å) must be subtracted from the instrument value (Grim, 1986; van Olphen, 1979). Displayed in Figure 21 is a typical diffractrogram. This is specifically the of DTMA-SAz-1 sample. From this data it was observed that the sample has a interlamellar spacing of 18.48601Å with an angle of 4.776 and an intensity of 53992. The average thickness was subtracted, resulting in an interlamellar spacing of 8.69 Å.

Table 12: Calculated interlamellar spacing of all four clays exchanged with all alkyl ammonium salts of interest as well as sodium ion, all in Å.

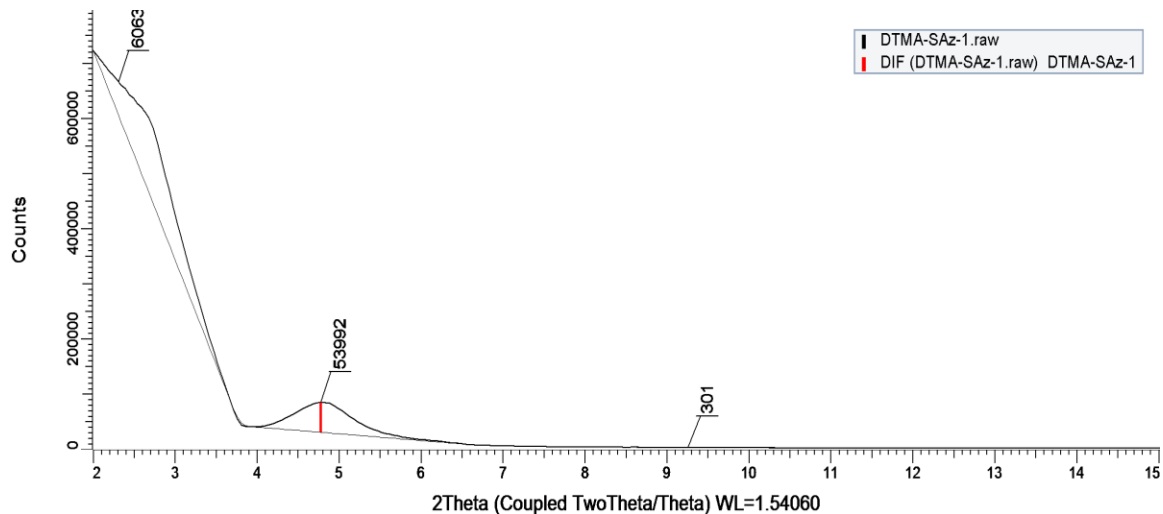| Salt \ Clays	SHCa-1	SWy-2	STx-1b	SAz-1
TEA	4.812	4.502	4.454	4.422
HTMA	4.221	4.211	4.168	4.339
PTMA	4.581	5.029	5.121	5.299
TPA	5.022	4.562	5.009	5.591
DTMA	4.827	4.358	5.899	8.686
MTBA	4.587	4.585	N/A	6.298
HDTMA	9.443	10.468	12.098	9.61
T.Pent	7.726	8.226	7.53	7.908
ODTMA	9.466	12.104	11.663	10.89
MTOA	14.888	12.547	12.16	4.698
Na^+ (neutral)	4.015	2.862	3.276	3.403

Figure 21: Diffractogram of DTMA-SAz-1. This is representative of all samples.
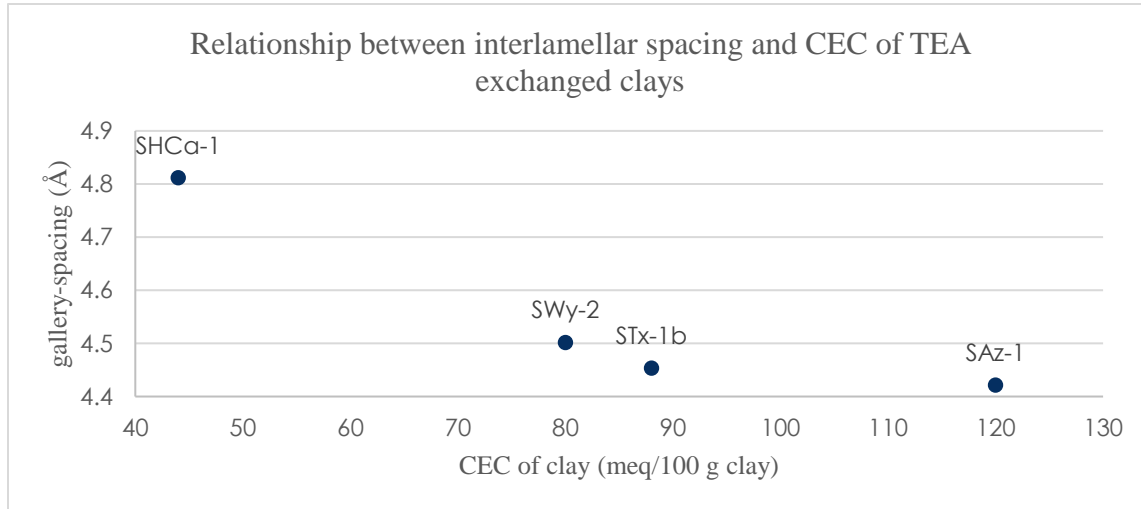

Figure 22: Visual representation of the relationship between interlamellar spacing and the accepted CEC of TEA exchanged clays.
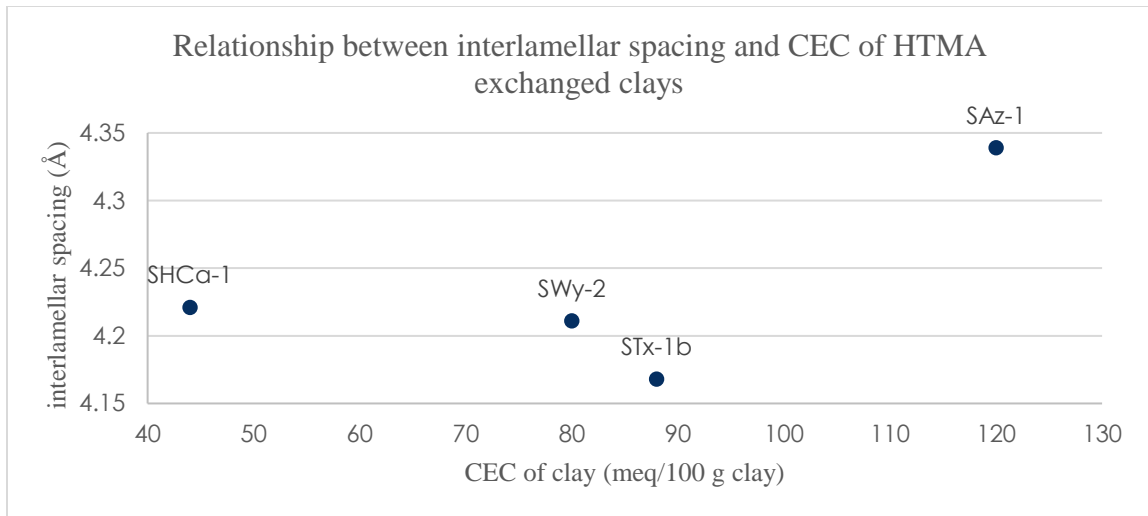
Figure 23: Visual representation of the relationship between interlamellar spacing and the accepted CEC of HTMA exchanged clays.

Figure 24: Visual representation of the relationship between interlamellar spacing and the accepted CEC of TPA exchanged clays.

Figure 25: Visual representation of the relationship between interlamellar spacing and the accepted CEC of MTBA exchanged clays.

Figure 26: Visual representation of the relationship between interlamellar spacing and the accepted CEC of PTMA exchanged clays.
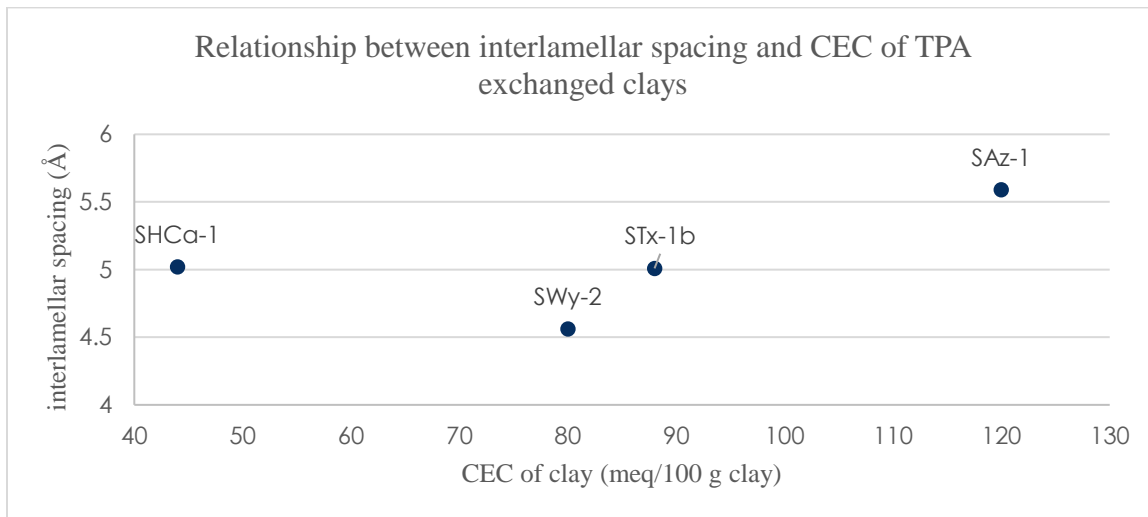
Figure 27: Visual representation of the relationship between interlamellar spacing and the accepted CEC of DTMA exchanged clays.

Figure 28: Visual representation of the relationship between interlamellar spacing and the accepted CEC of HDTMA exchanged clays.
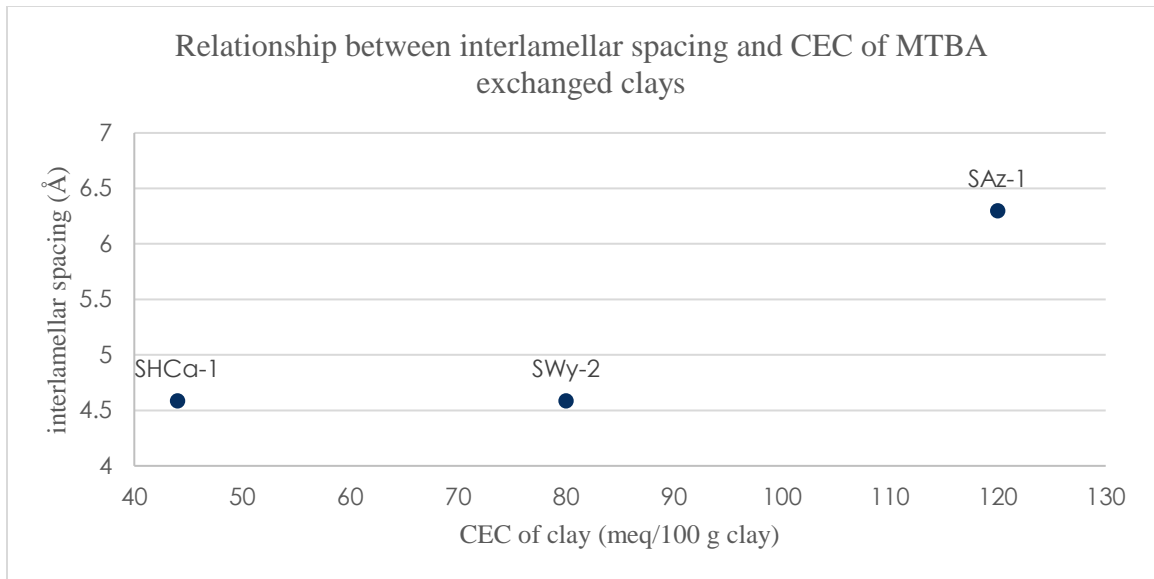
Figure 29: Visual representation of the relationship between interlamellar spacing and the accepted CEC of T. Pent exchanged clays.

Figure 30: Visual representation of the relationship between interlamellar spacing and the accepted CEC of ODTMA exchanged clays.

Figure 31: Visual representation of the relationship between interlamellar spacing and the accepted CEC of MTOA exchanged clays.
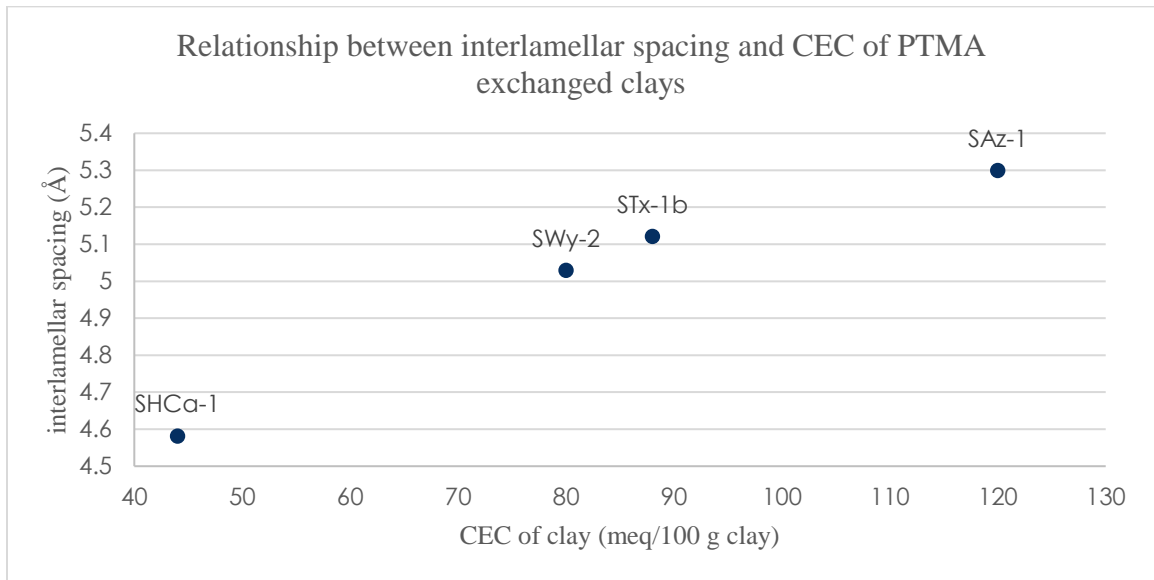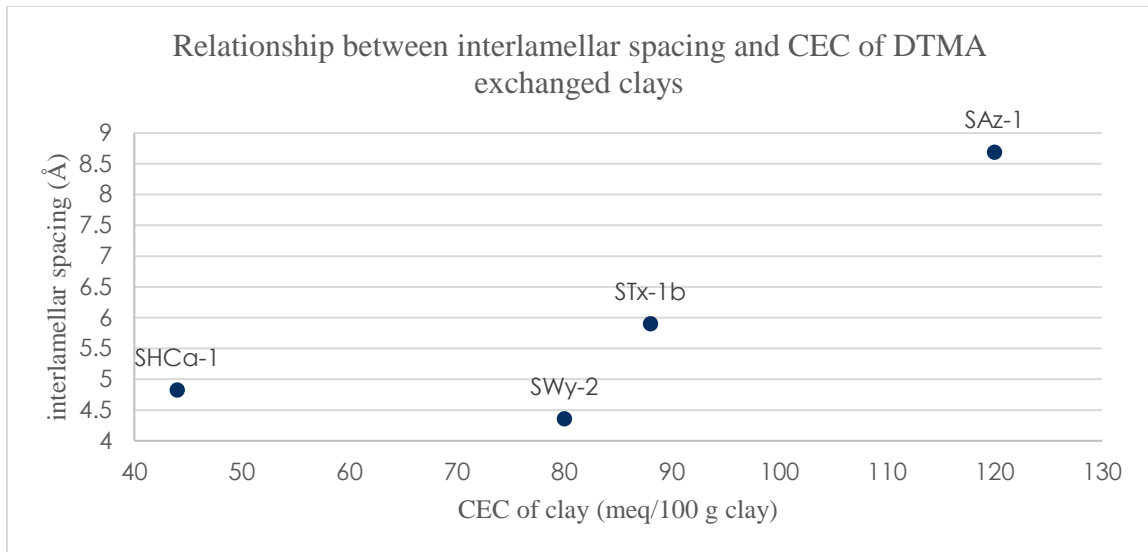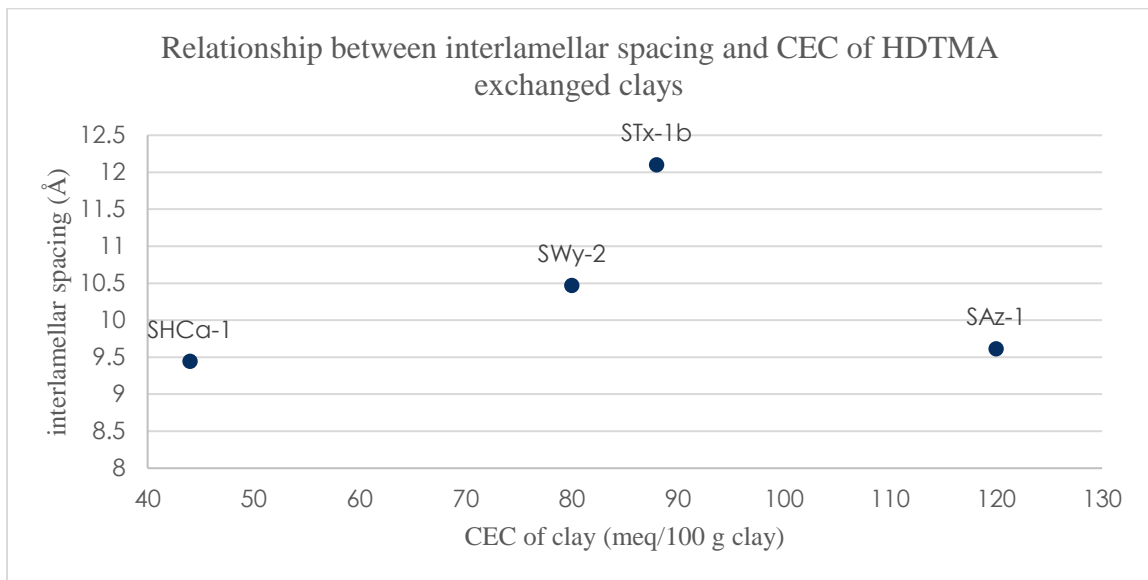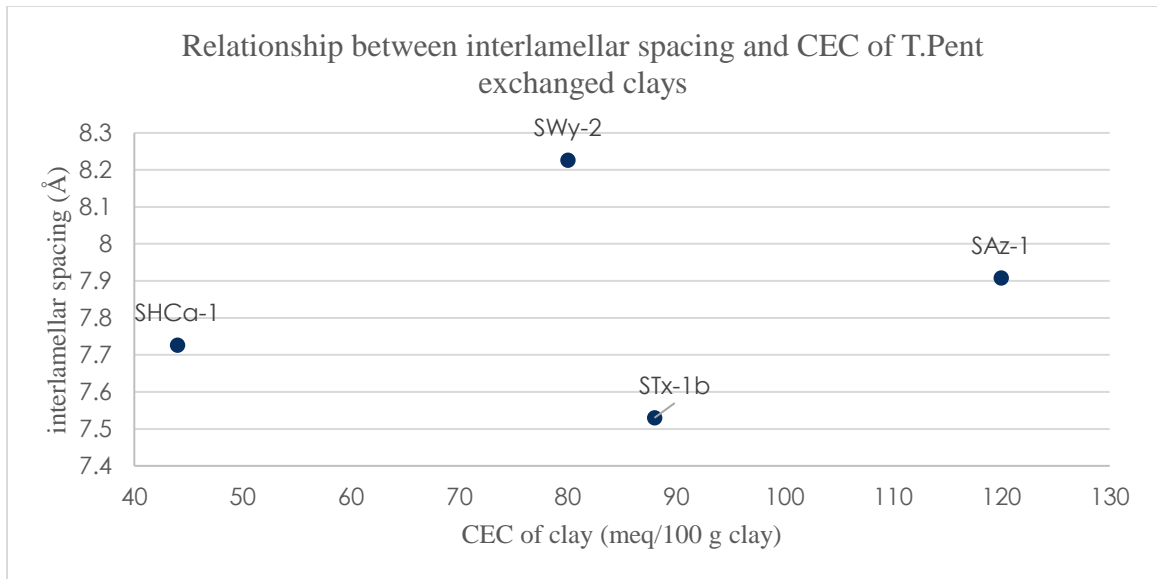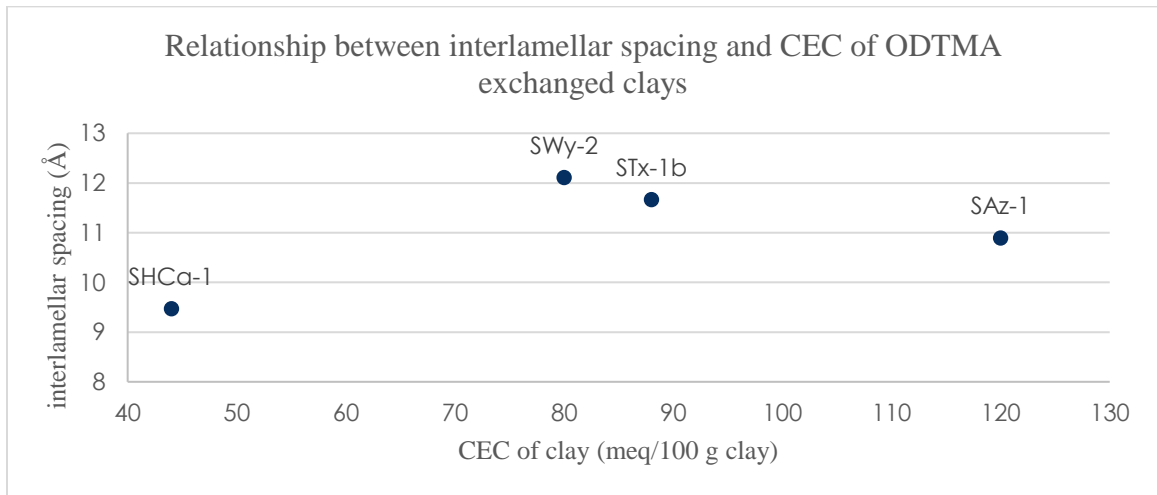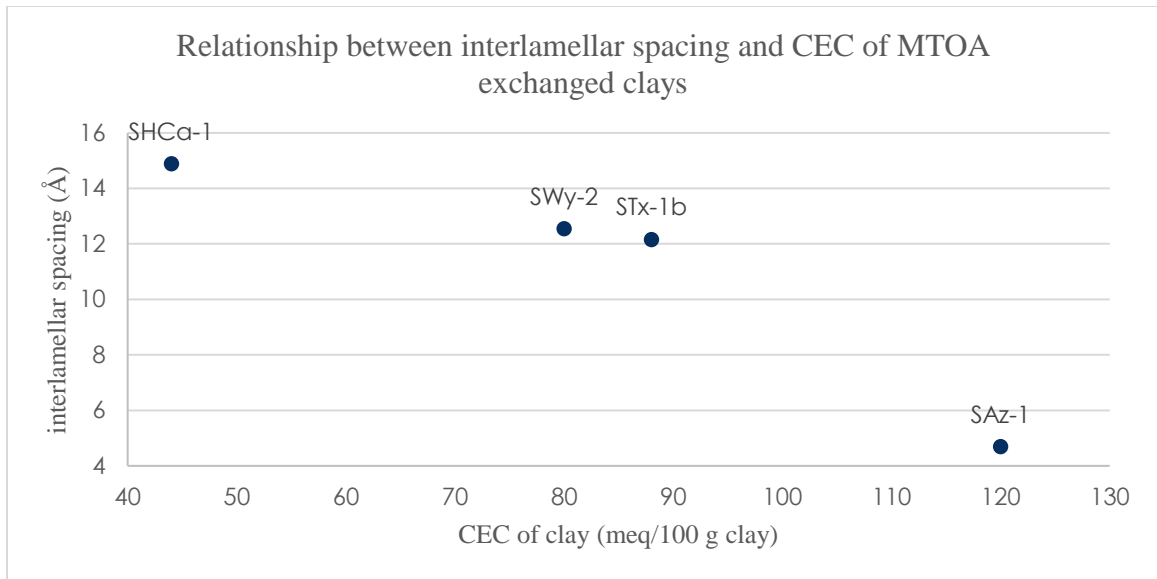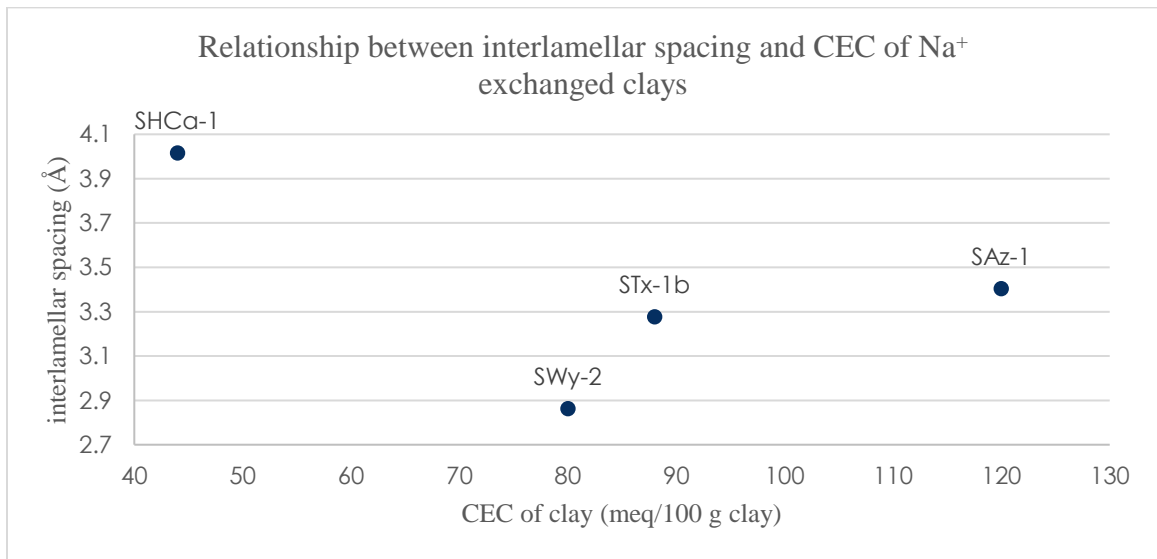

Figure 32: Visual representation of the relationship between interlamellar spacing and the accepted CEC of Na$^+$ exchanged clays.

The interlamellar spacing between the salt-clay samples seems to be unrelated, but when the spacing values for similarly substituted samples are examined (for example all of the tetra-substituted salts) a trend can be seen. Displayed in Figure 33 are the spacings for the tetra-alkyl ammonium-clay (TAA-clay) samples for SHCa-1.

Figure 33: Visual representation of average heat of combustion, and interlamellar spacing, with respect to number of carbons for tetraalkyl-SHCa-1.

Looking at just the gallery-spacing, there is a sharp increase as the number of carbons in increases. This trend suggests that pseudo layering is occurring in the interlamellar region of the clay where the long carbon chains are overlapping and spreading the layers apart rapidly. This same trend is seen in Figures 34, 35, and 36 for the tetraalkyl substituted salts with SWy-2, STx-1b, and SAz-1.
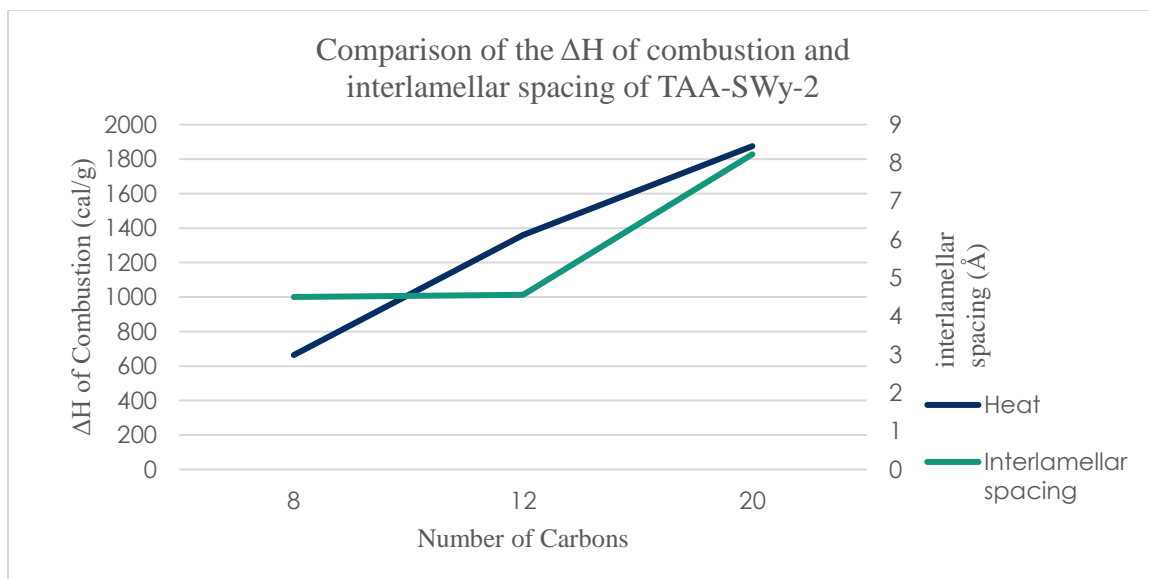
Figure 34: Visual representation of average heat of combustion, and interlamellar spacing, with respect to number of carbons for tetraalkyl-SWy-2.
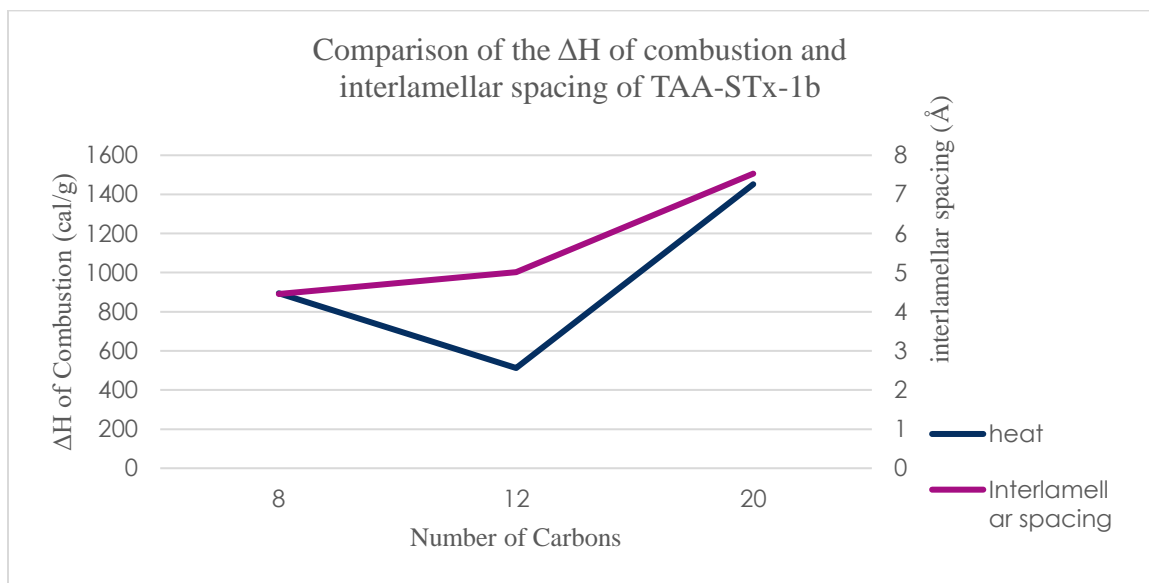
Figure 35: Visual representation of average heat of combustion, and interlamellar spacing, with respect to number of carbons for tetraalkyl-STx-1b.
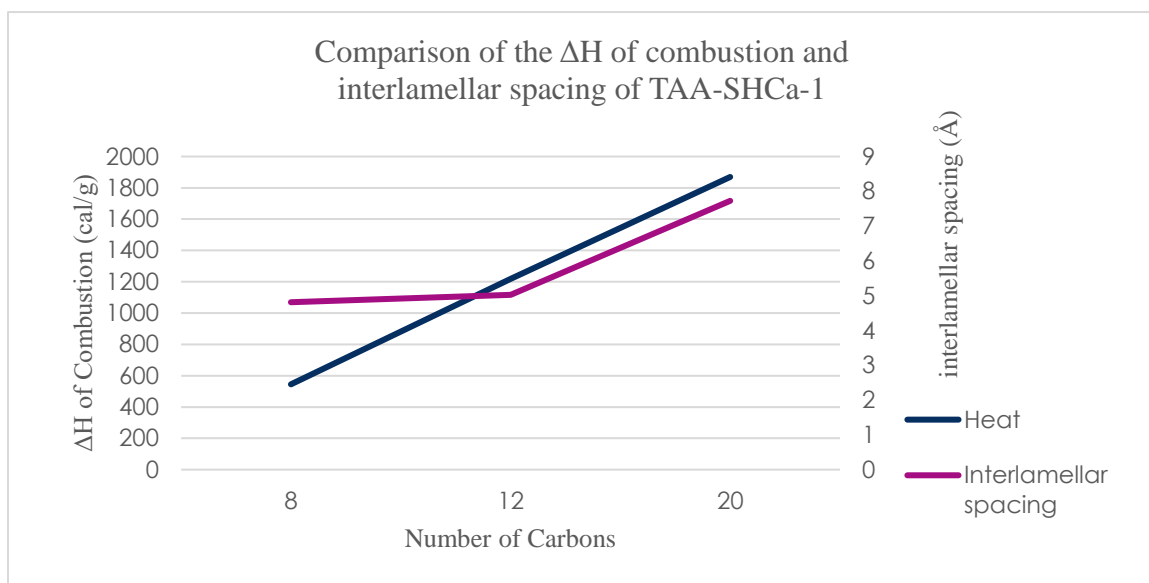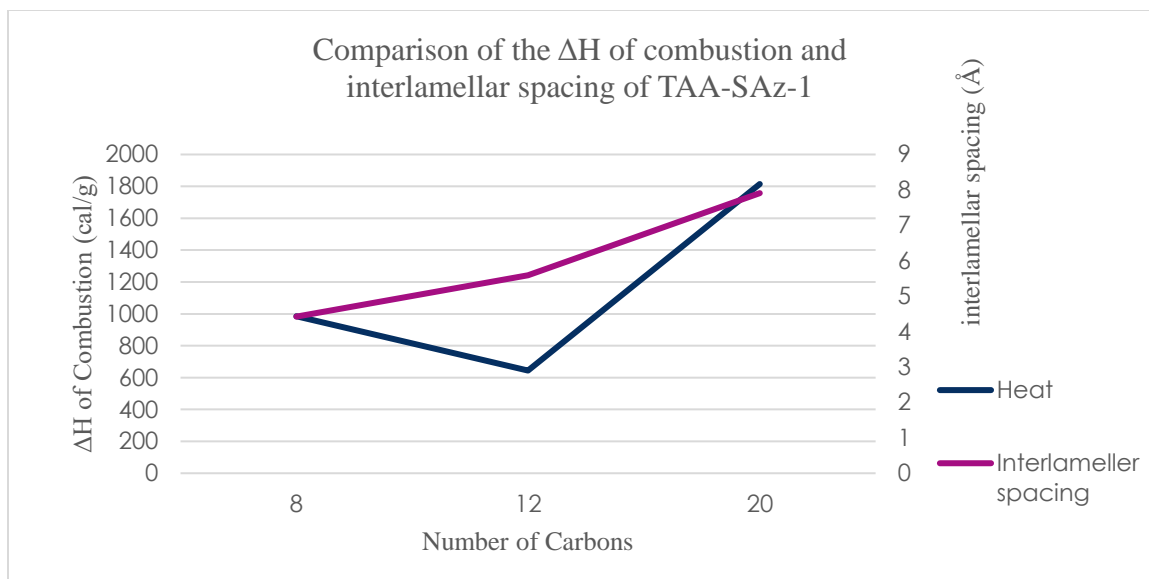
Figure 36: Visual representation of average heat of combustion, and interlamellar spacing, with respect to number of carbons for tetraalkyl-SAz-1.

Discussion

Overall, a positive trend is seen when comparing the heats of combustion and the known CEC of the clays for each salt. This supports the idea that the more charge sites a clay has (its CEC), the more alkyl ammonium salts the clay can accommodate. This is proof that the salts are interacting with the charge sites on the clay, which can ultimately lead to the determination of the CEC. One of the goals in this research was to determine which salt-clay combination yields the best results when compared to the ammonium electrode method, which has an error range of ±20%. The calculated CECs for each salt-clay combination are displayed in Tables 4-9. Some salts yielded very large percent

errors while others were smaller than the ±20% which strongly suggests those combinations are best suited for the CEC determination for that specific clay.

When comparing the percent errors for the calculated CECs of the four clays, HDTMA, and MTOA worked very well for SWy-1, STx-1b, and SAz-1. The clay with the lowest CEC of 44, SHCa-1, produced the lowest percent error with TEA which is the salt with the lowest number of carbons. The gallery-spacing of the Na^+ for each clay is the spacing of the interlamellar region containing only the sodium atom; before the introduction of the alkyl ammonium salt (seen in Table 11). This will be referred to as the neutral spacing of the clay for this research. The neutral spacing of the SHCa-1 is the largest which would theoretically lead to better accommodation of the alkyl ammonium salt during exchange especially when looking at the larger salts. This could potentially lead to better CECs. Seen in Table 5, the lowest percent error was for TEA, the smallest ion in this research, and the larger salts ranged from 29% to almost 600% error. The clay with the lowest neutral spacing, SWy-2, interacted with the larger salts very well when looking at the percent errors of the CEC. In fact, two of the lowest percent errors were the larger salts of HDTMA and MTOA. There is an obvious positive trend when looking at the spacing of all four clays as the number of carbons on the salt increases, which proves that the clay itself is adjusting to accommodate the molecules.

CHAPTER 5

Conclusion and Future Research

Bomb calorimetry was successfully used in the determination of the CEC of four smectite clays. In all four cases, this method yielded results with accuracy better than ±20%. The salt MTOA yielded acceptable accuracy for the clays SWy-2, STx-1b, and SAz-1 with all percent errors being less than 20%. Another salt that provided less than a 20% error for more than one clay was HDTMA. So, the goal to achieve CEC determination with a less than 20% error was successfully accomplished using bomb calorimetry. The clay SHCa-1 only had one exchanged sample less than 20%, TPA at 11.57%, all other samples were significantly higher. This is most likely due to a combination of sample size and CEC of the clay. The literature value of the CEC for SHCa-1 is 44 meq/100g clay and the sample size used in the semimicro vessel was around 0.2 g which made combustion difficult to achieve due to low concentration of hydrocarbon. Even with the problems encountered with SHCa-1, the use of bomb calorimetry in the determination of CEC was effective.

Further investigation on this topic would include the use of more salts similar to those that yielded the best results for each clay. Close examination of the substitution and distribution of the carbon chains around the central nitrogen atom (ex.: mono- ,di-. tri, etc.) would be incredibly useful when examining how the salts intercalate in the

interlamellar region of the clay. Organizing the salts in this manor instead of number of carbons would allow for a better comparison based on steric interactions. During this research, the biggest setback encountered was related to sample size; there was not enough hydrocarbon present to facilitate a combustion reaction. A solution to this would be to increase sample size of the exchanged salt ensuring that sufficient materials for combustion. Running all samples on the standard bomb calorimeter would allow sample sizes of up to 0.8 g to be analyzed as opposed to the maximum of 0.2 g with the semi micro bomb calorimeter. An increase in sample size would result in a longer purification process to generate enough clay for exchange. The increase in sample size would lead to less spiking of the samples ultimately lowering the standard deviation.

REFERENCES

1.   Borden, D., Baseline Studies of the Clay Minerals Society Source Clays: Cation Exchange Capacity Measurements by the Ammonia Electrode Method. Clays and Clay Minerals 2001, (49.5), 444-445.

2.   Busenberge, E.; Clemency, C. V., Determination Of the Cation Exchange Capacity of Clays and Soils Using an Ammonia Electrode. Clays and Clay Minerals 1973, 21, 213-217.

3.   Duane, M.; Reynolds, R., X-ray Diffraction and the Identification and Analysis of Clay Minerals. Oxford UP 1997, (2).

4.   Emam, E. A. ARPN Journal of Science and Technology 2013, 3 (4), 356–375.

5.   Fernandez Gonzalez, M.; Lagaly, G.; Weiss, A., Problems in Layer-Charge Determination of Montmorillonites. Clay Minerals 1976, (11), 173-187.

6.   Hectorite Mineral Data. In Webmineral. http://webmineral.com/data/Hectorite.shtml#.Wz2aLtJKjIU

7.   Indarawis, K., Alkaline Earth Metal Cation Exchange: Effect of Mobile Counterion and Dissolved Organic Matter. Environmental Science & Technology 2012, 48.6, 4591-4598.

8.   Kloprogge, T. J., Synthesis Of Smectite Clay Minerals: A Critical Review. Clays and Clay Minerals 1999, (47), 529-554.

9.   Lagaly, G., Layers Charge Determination by Alkylammonium Ions. Layer Charge Characteristics of 2:1 Silicate Clay Minerals 1994, 6, 2-46.

10.   Mermut, A., Baseline Studies of the Clay Minerals Society Source Clays: Layer-Charge Determination and Characteristics of Those Minerals Containing 2:1 Layers. Clays and Clay Minerals 2001, 49.5, 393-397.

11.   MilliporeSigma, United States https://www.sigmaaldrich.com/united-states.html (accessed Jul 5, 2018).

12.   Newman, A. C. D., Chemistry of Clays and Clay Minerals. Wiley: New York, 1987.

13.   Odem, I. E., Smectite Clay Minterals: Properties and Uses. Philosophical Transations of the Royal Society of London 1984, 391-409.

14.   Parr, Operations Manual for the 1109/1109A Semi-Micro Oxygen Bombs. 2007, 493M.

15.   Parr, Operation Instructions Manual 6772 Calorimetric Thermometer. Parr: 2008; Vol. 483M.

16.   Perrin, J. Steric Considerations in the Combustion of Organo-Clays. SFASU, Nacogdoches, 2009.

17.   Poppe, L. J. A laboratory manual for x-ray powder diffraction; U.S. Geological Survey, Coastal and Marine Geology Program: Woods Hole, MA, TX, 2001.

18.   Rich, A. D. A Thermodynamic Study of Cation Exchange in Montmorillonite Clays Using Solution Calorimetry. Stephen F. Austin State University, Nacogdoches, 2009.

19.   Rodriguez-Reinoso, F. Characterization of Porous Solids II, Proceedings of the IUPAC Symposium (COPS 11) Studies in Surface Science and Catalysis 1991, 11, 771-773.

20.   Steinmetz, D. R. Texture evolution in processing of polystyrene-clay nanocomposites. thesis, 2007.

21.   Teich-McGoldrick, S. L.; Greathouse, J. A.; Jové-Colón, C. F.; Cygan, R. T. The Journal of Physical Chemistry C 2015, 119 (36), 20880–20891.

22.   van Olphen, H.; Fripiat, J. J. Data Handbook for Clay Minerals and Other Non-Metallic Minerals. Soil Science 1979, 131.1, 346.

VITA

After graduating high school in 2016, Celeste Keith moved from Santa Fe, Texas to attend Stephen F. Austin State University. She graduated with a Bachelor of Science in Chemistry in May 2016, then enrolled in Graduate School at SFASU and graduated with a degree of Master of Natural Science in August 2018. During her graduate work, she worked as a laboratory teaching assistant and stockroom assistant.

Permanent Address: 3030 Cemetery Rd.

Santa Fe, TX 77517

Style manual designation: American Chemical Society (ACS) Style Guide

This thesis was typed by C.A. Keith